photonics

MDPI

Review

A Review of Light-Emitting Diodes and Ultraviolet Light-Emitting Diodes and Their Applications

Trailokya Bhattarai [1,*], Abasifreke Ebong [1] and Mohammad Yasin Akhtar Raja [2]

[1] Department of Electrical Engineering and Computer Science, UNC Charlotte, Charlotte, NC 28223, USA; aebong1@uncc.edu
[2] Department of Physics and Optical Science, UNC Charlotte, Charlotte, NC 28223, USA; raja@uncc.edu
* Correspondence: tbhattar@uncc.edu

Abstract: This paper presents an extensive literature review on Light-Emitting Diode (LED) fundamentals and discusses the historical development of LEDs, focusing on the material selection, design employed, and modifications used in increasing the light output. It traces the evolutionary trajectory of the efficiency enhancement of ultraviolet (UV), blue, green, and red LEDs. It rigorously examines the diverse applications of LEDs, spanning from solid-state lighting to cutting-edge display technology, and their emerging role in microbial deactivation. A detailed overview of current trends and prospects in lighting and display technology is presented. Using the literature, this review offers valuable insights into the application of UV LEDs for microbial and potential viral disinfection. It conducts an in-depth exploration of the various microorganism responses to UV radiation based on the existing literature. Furthermore, the review investigates UV LED-based systems for water purification and surface disinfection. A prospective design for a solar-powered UV LED disinfection system is also delineated. The primary objective of this review article is to organize and synthesize pivotal information from the literature, offering a concise and focused overview of LED applications. From our review, we can conclude that the efficiency of LEDs has continuously increased since its invention and researchers are searching for methods to increase efficiency further. The demand for LED lighting and display applications is continuously increasing. Our analysis reveals an exciting horizon in microbial disinfection, where the integration of UV LED systems with cutting-edge technologies such as sensors, solar power, Internet-of-Things (IoT) devices, and artificial intelligence algorithms promises high levels of precision and efficacy in disinfection practices. This contribution sets the stage for future research endeavors in the domain of viral disinfection using solar-powered UV LED modules for universal applications.

Keywords: LED fundamentals; LED history; LED efficiency; UV LED; blue LED; green LED; red LED; white lighting; lighting and display applications; mini-LED; micro-LED; microbial deactivation; UV dose; solar powered UV LEDs

check for updates

Citation: Bhattarai, T.; Ebong, A.; Raja, M.Y.A. A Review of Light-Emitting Diodes and Ultraviolet Light-Emitting Diodes and Their Applications. *Photonics* **2024**, *11*, 491. https://doi.org/10.3390/photonics11060491

Received: 11 April 2024
Revised: 14 May 2024
Accepted: 15 May 2024
Published: 22 May 2024

Copyright: © 2024 by the authors. Licensee MDPI, Basel, Switzerland. This article is an open access article distributed under the terms and conditions of the Creative Commons Attribution (CC BY) license (https://creativecommons.org/licenses/by/4.0/).

1. Introduction

Light-Emitting Diodes (LEDs) are primarily p-n junction-based devices made of direct bandgap semiconductors and emit light when an electric current is injected into the device [1]. The choice of a particular semiconductor material (direct bandgap) is essential to achieve the required wavelength. The wavelength of the emitted light is a function of the bandgap, i.e., $\lambda = hc/E_g$. LEDs comprise very thin layers of semiconductor materials and the layers are quite heavily doped. When forward-biased, these emit light at characteristic wavelengths, depending on the semiconductor material used. Figure 1 shows a schematic of a LED with basic working principles.

Oleg Vladimirovich Losev, an influential Russian scientist, played a pivotal role in advancing semiconductor electronics through his discovery of electroluminescence [2]. His groundbreaking research, conducted in the early 1920s using materials such as silicon

carbide (SiC) crystals, led to a deep understanding of how electrical charges interact within these substances to produce light. Losev's findings laid the groundwork for the development of modern LED lights, which have entered widespread use in everyday items like lamps and screens. Additionally, Losev's thorough investigation into injectional and prebreak down luminescence effects contributed significantly to the field, which led to in his receipt of the first patent for a pre-sample to the light-emitting diode in 1927 [3].

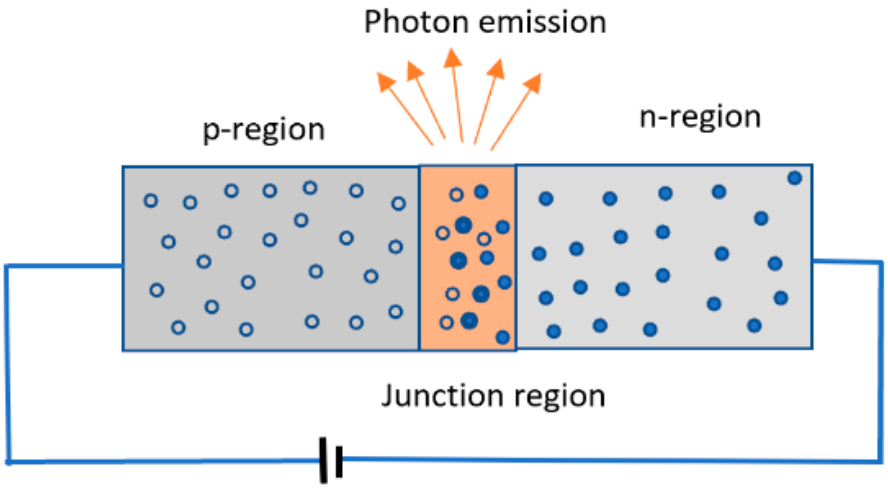


Figure 1. Basics of LED structure and photon emission.

In general, there are no elemental direct bandgap materials, but compound semiconductors such as GaAs, GaP, GaN, and similar others have direct bandgaps. Depending on the energy bandgap, the emitted light will vary in wavelength, ranging from UV to infrared. Figure 2 displays device wavelengths, frequency, and material bandgap for the emission of UV, blue, green, and red light. Table 1 displays the growth method, material combination, and the p-n junctions required for the emission of UV, blue, green, and red light.

The development of materials for LEDs has played a crucial role in the advancement of this technology. LEDs have come a long way since their invention, and there is continuous research into the improvement in the materials used for their fabrication. Earlier challenges in making efficient LEDs were primarily related to the materials and structures used in their design. Initially, LEDs faced issues of a low extraction efficiency due to the absorbing substrates used, limiting the amount of emitted light [4]. The development of GaN-based materials in the late 1980s and early 1990s marked a significant breakthrough in enhancing the efficiency of solid-state light emitters, including LEDs [5]. GaN is a fundamental material in LED technology, serving as the basis for almost all commercial LEDs due to its wide bandgap and efficient light emission properties [6]. AlGaN, an alloy of aluminum and gallium nitride, is commonly used in deep ultraviolet LEDs, although issues related to optical power degradation have been observed over time [7]. Magnesium Oxide (MgO), 7.8 eV [8], is a key component in photonics and LED due to its unique properties. In photonics, MgO is commonly used as a substrate material for thin-film photovoltaics, LEDs, and solid-state lasers, providing exceptional optical and electrical characteristics. MgO, commonly used as a buffer layer in GaN LED structures, has been shown to enhance device performance and reliability by reducing dislocation density and improving thermal management [9]. Epitaxial lateral overgrowth (ELO) is a semiconductor growth technique aimed at reducing defects, particularly threading dislocations, in epitaxial layers. In ELO, a thin seed layer is deposited on a substrate, and growth is initiated from this layer. According to Malinauskas et al. [10] the contribution of dislocations to carrier recombination and transport in highly excited ELO and HVPE GaN layers has been investigated. These layers exhibit distinct dislocation densities, with ELO layers typically having lower densities compared to HVPE layers. Under high-excitation conditions, dislocations act as significant centers for carrier recombination, leading to variations in carrier lifetimes and transport

properties. Thus, understanding this contribution is crucial for optimizing the performance of GaN-based devices. Also, the defect densities in GaN can be reduced using one- or two-step epitaxial lateral overgrowth methods [11,12].

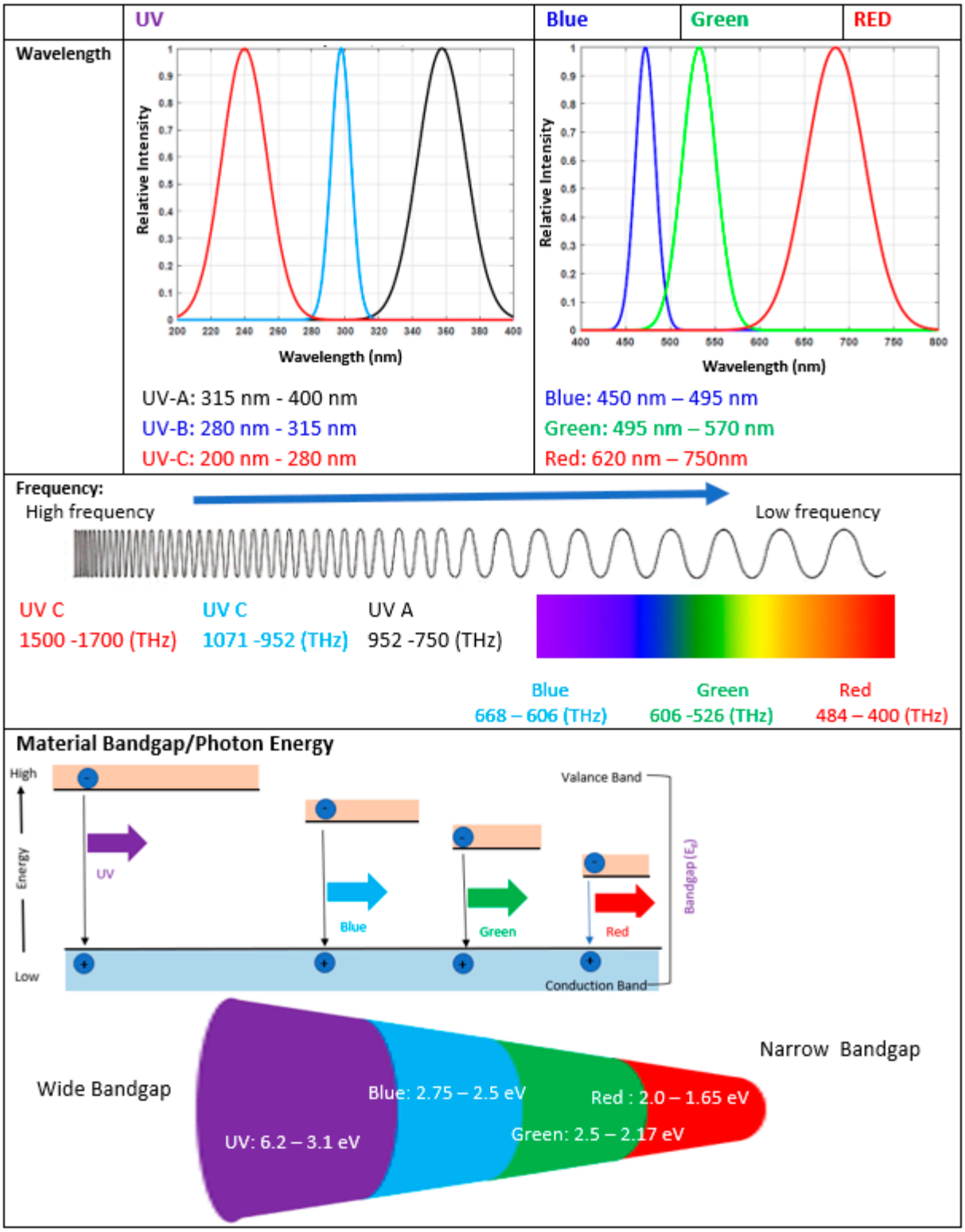


Figure 2. Figure showing the wavelength, frequency, and bandgap of UV, blue, green, and red light.

Table 1. Illustrations of the growth method, material combination, and the p-n junctions used for the emission of UV, blue, green, and red light.

	UV	Blue	Green	Red
Growth Method	• MOCVD (Metal Organic Chemical Vapor Deposition) [13] • MBE (Molecular Beam Epitaxy) [14,15] • PVD (Physical Vapor Deposition) [16] • Solution-based methods (such as spin-coating or inkjet printing) [17] • HVPE (Hydride Vapor-Phase Epitaxy) [18] • PAMBE (Plasma-Assisted Molecular Beam Epitaxy) [19] • MBE-MOVPE hybrid approach [20]	• MOCVD [21,22] • MBE [23] • PVD [16] • HVPE [18] • MBE-MOVPE hybrid approach [20] • LPE (Liquid-Phase Epitaxy) [24]	• MOCVD [22] • MBE [23] • PVD [16] • Hybrid approaches [20] • MOVPE (Metal Organic Vapor-Phase Epitaxy) [25] • VPE (Vapor-Phase Epitaxy) [26]	• MOCVD [13] • MBE [23] • PVD [27]
Group-Combination (II, III, V, VI)	• III-V materials: [28] AlGaN, AlGaInN • II-VI materials [29]: ZnO, MgO	• III-V materials [28]: GaN, InGaN, AlGaN • II-VI materials [30]: ZnSe, CdSe	• III-V materials [28]: InGaN, AlGaInP	• III-V materials: GaAs, AlGaAs, InGaP [31]
Type of Junctions Used in fabrication	• Double heterojunction (DH) junction [32] • Multiple Quantum well (MQW) Junction [33] • Zinc oxide (ZnO) homojunction [34] • Aluminum gallium nitride (AlGaN) heterojunction [35]	• DH junction [32] • MQW Junction [33] • ZnSe homojunction [36] • InGaN heterojunction	• DH junction [32] • MQW Junction [33] • Single hetero [SH] junction [37] • ZnO homojunction [34]	• DH junction [32] • MQWs Junction [33] • SH junction [37] • Zinc oxide (ZnO) homojunction [34]

Thus, the selection of materials for LEDs requires careful consideration of various factors to ensure optimal performance. Researchers face challenges in material selection due to the need for high efficiency, stability, and cost-effectiveness. Different materials such as organic compounds, quantum dots, perovskites, and nanocrystals are being explored for their potential in LED applications [38–40]. Challenges include ensuring lattice matching between different layers, achieving high brightness, and addressing issues like material degradation over time [41]. To overcome these challenges, researchers are focusing on innovative solutions such as surface treatments to enhance efficiency, utilizing hybrid materials to improve performance, and developing new fabrication techniques to optimize the properties of the materials used [42–44]. By combining the unique properties of various materials and continuously refining the manufacturing processes, researchers aim to create LEDs that are not only highly efficient but also durable and cost-effective [45–47]. Additionally, advancements in the material, such as the development of new host materials and charge transport layers, are contributing to the improvement in LED technology [48,49]. Overall, the ongoing research in material selection for LEDs is focused on overcoming existing challenges and pushing the boundaries of efficiency and performance in lighting technology.

Earlier designs in LED structures prioritized effective thermal management to ensure the reliability and longevity of LED systems [50]. It was dedicated to managing thermal paths and packaging for LEDs to address challenges related to higher electrical currents and heat dissipation [51]. The structural configurations of LEDs was focused on balancing compact, efficient internal layouts, and the management of heat density [52]. Researchers also investigated the influence of structural arrangements on controlling LED junction temperature, showing the importance of proper design considerations in this aspect [53]. The development of LED structures with improved thermal properties was a key focus, leading to advancements in thermal simulation and measurement techniques [54].

The recent developments in LED design include the integration of quantum dots (QDs) into LED structures, resulting in the creation of highly efficient inverted structure

QD-based LEDs [43]. Recent research has also investigated the incorporation of flaw-containing alumina hollow nanostructures to improve fracture strength in GaN LEDs [55]. These breakthroughs signify a move towards designing LED structures with greater efficiency and output capacities, opening up possibilities for innovative applications across various domains.

Various methods of deposition are utilized in the fabrication of LEDs to achieve better optimal performance. MOCVD has been widely employed for LED growth, providing conditions conducive to device development [13]. MOCVD has been employed in the growth of GaN-based LED structures on various substrates, including sapphire and silicon, to achieve different emission wavelengths [22]. MBE is known for its ability to produce high-quality epitaxial layers, as seen in the investigation of ZnO (3.37 eV) layers [56,57]. MOVPE has been used in the growth of GaN core/shell wires for LED applications on silicon substrates [58]. LPE is another method employed in LED fabrication, offering the potential for the growth of multi-layer structures like $InAs/InAs_xP_{1-x-y}Sb_y/InAs/InAs_{x'}P_{1-x'-y'}Sb_{y'}$ [59]. VPE methods such as MOVPE and HVPE have been extensively utilized in the production of high-quality semiconductor films and nanostructures [60]. In summary, the choice of deposition method in LED fabrication is crucial in determining the performance and characteristics of the devices. Each technique, whether it be MOCVD, MBE, LPE, or MOCVD, offers distinct advantages that can be harnessed to tailor LEDs for specific applications.

LEDs have a wide range of applications from lighting, displays, and decorations to microbial disinfections. In this review paper, we discuss an evolutionary history of UV-to-visible (blue, green, and red) LEDs and their applications. Moreover, their contemporary and future trends are reviewed. We have left out the IR group of LEDs for brevity.

In Section 2, we focus on the evolutionary history of each color starting from UV to red, mimicking the wide-to-narrow energy bandgap, although historically IR and red LEDs precede the decades before UV was realized. Section 3 discusses the status and prospects of LED lighting technology, whereas Section 4 reviews the application of LEDs in display technology. In the ongoing discussion, Section 5 provides a detailed analysis of the applications of UV-LEDs in the disinfection and cleansing processes. Here, a detailed study of the microbial disinfection of water and those of diverse surfaces is presented a bit more thoroughly. Further, in Section 6, we present a way forward in designing an efficient disinfection system and its future development in the cleansing applications. We also present a design of a UV LED system applicable to microbial deactivation. Finally, Section 7 includes the discussion and concluding remarks on the future of LED applications and is followed by the references to the pertinent literature.

2. Evolutionary History of LEDs

Reviewing a wide variety of published works in the literature, a chronological history of efficiency and efficacy developments of UV, blue, green, and red LEDs emerged in our study. Infrared LEDs are deliberately omitted to keep the paper concise and manageable as well as reader friendly.

2.1. Evolution of UV LEDs

The development of UV LEDs was motivated by applications such as fluorescence-based chemical sensing, high-efficiency lighting, flame detection, disinfection, optical storage, and countless more. Most of these applications require deep UV wavelengths around 300 nm. However, the ease of fabrication of UV LEDs is a function of the approximate wavelength required. Thus, the relatively shorter wavelengths are more challenging in engineering the bandgap. In general, UV LEDs at shorter wavelengths require Al contents at a higher fraction. However, the wide bandgap (high Al content) can result in high dislocation density and make the material less efficient. Thus, an optimized amount of Al is required to obtain the appropriate wavelength. In this section, we will review the evolution of the efficiency of UV LEDs in two regimes of wavelengths: (i) above 300 nm

and (ii) below 300 nm. We start with the above-300 nm regime because it is relatively easy to fabricate.

2.1.1. UV—Wavelengths Longer than 300 nm

Figure 3 shows a data point for the first ever reported UV LED at a 375 nm wavelength developed by Akasaki et al. [61] in 1993, with an efficiency of 1.5%. The structure of this first UV LED was based on the understanding of the mechanism of heteroepitaxial growth by MOVPE and hydride vapor phase epitaxy (HVPE) on a highly mismatched substrate. This enabled them to grow high-quality nitride films on various substrates such as α-Al_2O_3; thus, the epi-structures, GaN/AlN/α-Al_2O_3 layers, were grown.

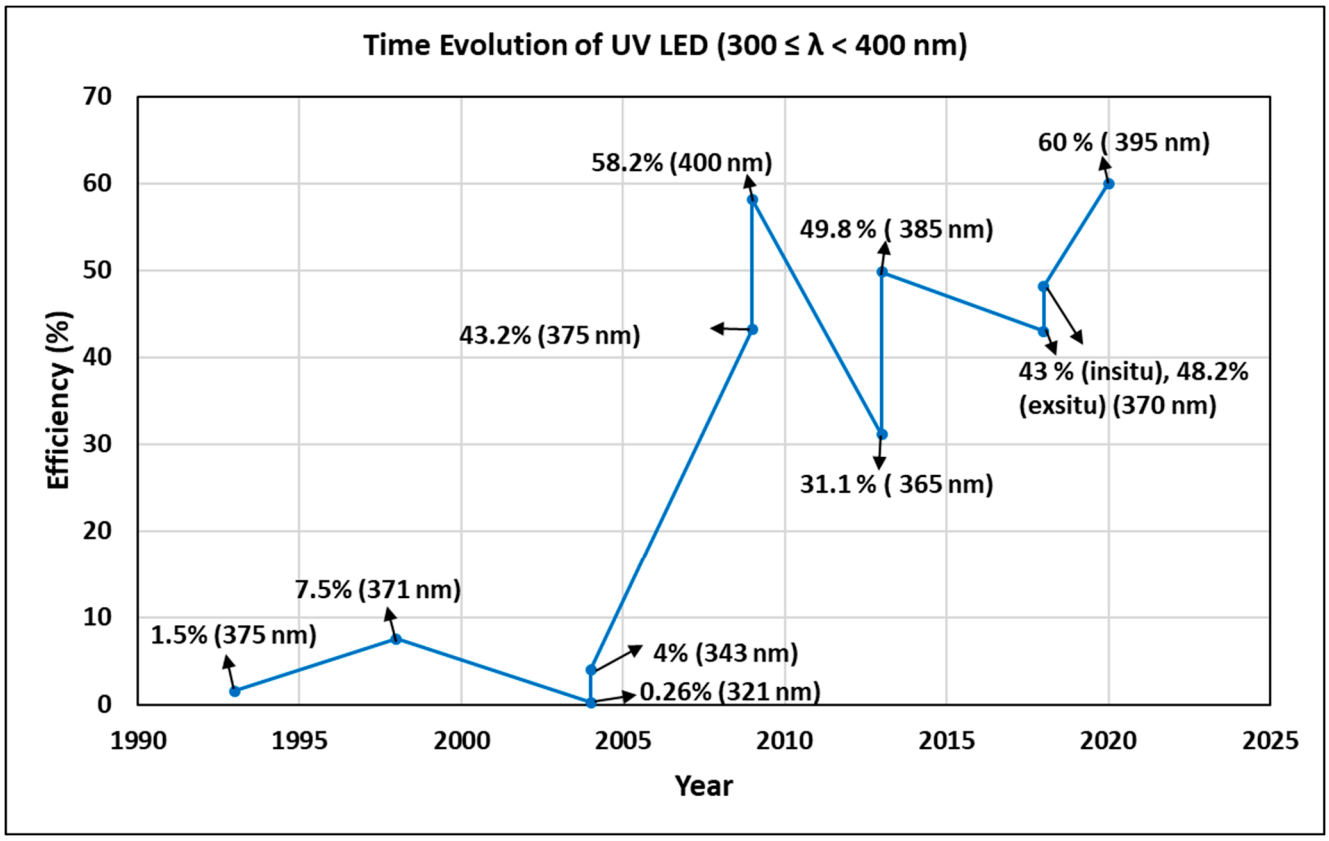


Figure 3. Time evolution of UV LED (≥300 nm) with respect to efficiency [32,61–65].

In 1998, Mukai et al. [32] reported a 7.5% efficiency UV LED at 371 nm with an addition of undoped InGaN, as shown in Figure 4. The undoped InGaN layer serves as a buffer layer to reduce lattice mismatch, a diffusion barrier, and also as a stress buffer, thereby improving the performance and reliability of the LEDs. The p-GaN/AlGaN/InGaN DH structures were grown by MOCVD. A DH structure improves efficiency by confining carriers to the active region (potential well), reducing non-radiative recombination at the interfaces, and increasing the probability of radiative recombination.

In a quest to obtain relatively shorter wavelengths, in 2004 Edmond et al. [62] reported 0.26% efficient UV LED at 321 nm and 4% at 343 nm. Their structure featured an n-type GaN layer followed by an MQW stack consisting of n-AlGaN/AlGaN/n-AlGaN layers and then a thin p-GaN contact layer. The MQWs improve performance and efficiency by confining charge carriers to a narrow region, enhancing the probability of radiative recombination, thereby reducing non-radiative recombination, and allowing for precise control over emission wavelength and efficiency.

The challenges during that time were increasing efficiency and keeping the wavelength short. Thus, in an effort to increase efficiency, Muramoto et al. [63], in 2009, fabricated UV

LEDs with an efficiency of 43.2% at 375 nm and 58.2% at 400 nm, respectively., They used a GaN buffer layer and AlGaN active layers. Later, in 2013, to achieve shorter wavelengths, the same research group was able to improve the efficiency to 31.3% for 365 nm and 49.8% for 385 nm, respectively. They achieved this by decreasing the dislocation density, increasing the variation in In composition, and decreasing UV absorption by the GaN buffer layer. Also, they had changed their structure from face-up LED to vertical chip LED, as shown in Figure 5. One of the main benefits of vertical chip LEDs over face-up LEDs is that they offer better heat dissipation, resulting in improved reliability, longer lifespans, and higher light outputs.

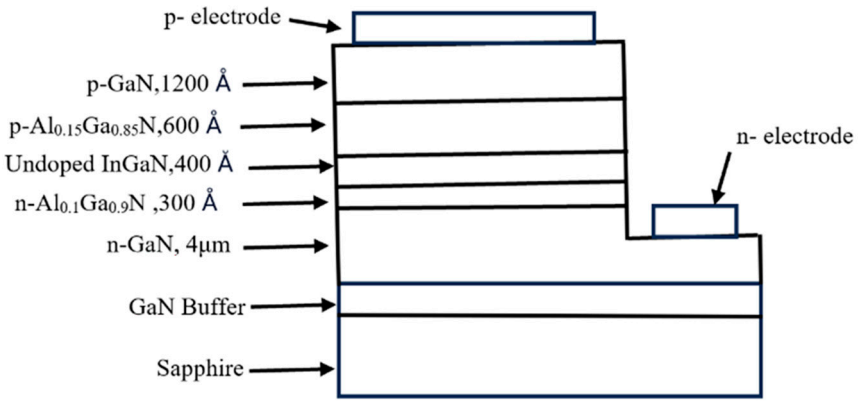


Figure 4. InGaN/AlGaN DH UV LED structure.

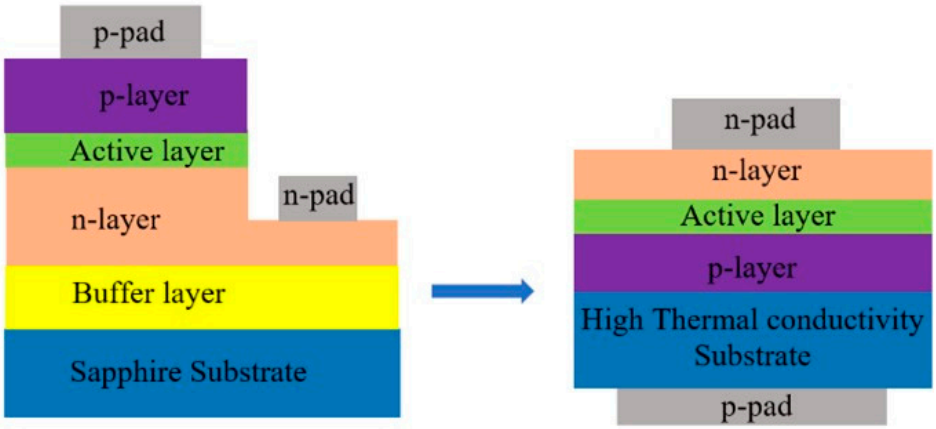


Figure 5. LED structure diagram (**left**: face-up LED, **right**: V-chip LED) [Substrate: sapphire; buffer layer: GaN; n-layer: n-GaN; active layer: AlGaN/AlInGaN/AlGaN DH layers; p-layer: p-GaN].

The quest for the fabrication of a higher efficiency and power output in UV LEDs continuously kept on growing. In 2018, Tak Oh et al. [64] compared the performance of GaN-based UV vertical LEDs (VLED) grown on 6-inch sapphire substrates. They used an ex situ sputtered AlN nucleation layer and an in situ low-temperature AlGaN nucleation layer. The maximum external quantum efficiency (EQE) of the Vertical LED at 370 nm with the in situ AlGaN and ex situ AlN were 43.7% and 48.2%, respectively [64]. The ex situ AlN samples showed relatively lower densities of threading dislocations and were under more compressive stress than the in situ AlGaN samples. The packaged LEDs with the ex situ AlN nucleation layer had a higher light output power and maximum efficiency than the in situ AlGaN-nucleation-layer LEDs. The improved performance of the ex situ AlN sample was attributed to the lower density of threading dislocations. Those were some of the highest efficiencies achieved for UV LEDs to that date.

Further, in 2020, a research group, Li et al. [65], were able to design UV LEDs of an efficiency of 60% at a wavelength of 395 nm. Their design consisted of epitaxial layers on

4-inch Si substrates, and they grew AlN, AlGaN, and undoped GaN buffer layers. A 3 µm thick n-type GaN layer, 9-period MQWs (AlGaN/GaN/InGaN), and an electron-blocking layer (EBL) were grown on a 200 nm thick p-type GaN layer. The introduction of the GaN interlayer barrier improved the concentration and spatial overlap of the carriers in the MQWs, which led to the modulation of the energy band and polarization, resulting in enhanced efficiency. The design of their structure is shown in Figure 6.

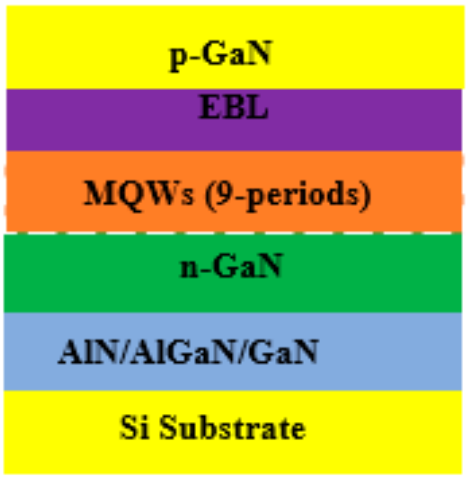


Figure 6. The epitaxial structures for 60% efficient UV LED (λ = 395 nm).

2.1.2. UV—Wavelength Shorter than 300 nm

In the early 2000s, the fabrication of UV LEDs emitting wavelengths shorter than 300 nm was highly challenging due to the need for materials with larger bandgaps. These materials were scarce and more difficult to manipulate compared to those used in longer-wavelength LEDs, and the shorter wavelengths were prone to absorption and scattering by impurities, leading to reduced LED efficiency. Figure 7 displays a 'Time Evolution' of a UV LED (<300 nm) with respect to efficiency.

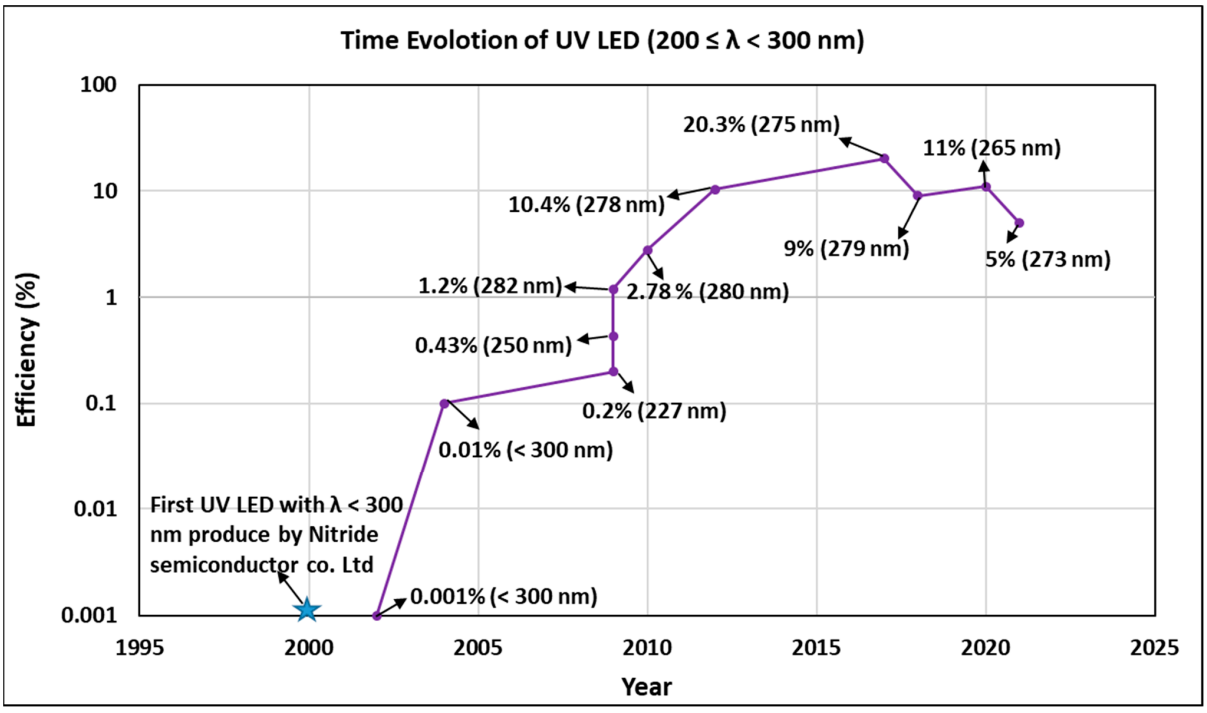


Figure 7. Time evolution of UV-LED (<300 nm) with respect to efficiency [66–72].

The first <300 nm UV-LEDs were fabricated by Nitride Semiconductor Co. in Tokushima, Japan in collaboration with the University of Tokushima in April of 2000 [63]. The basic design of those LEDs is shown in Figure 8. However, the achieved efficiency for those UV-LEDs was quite low and was not even mentioned by the authors.

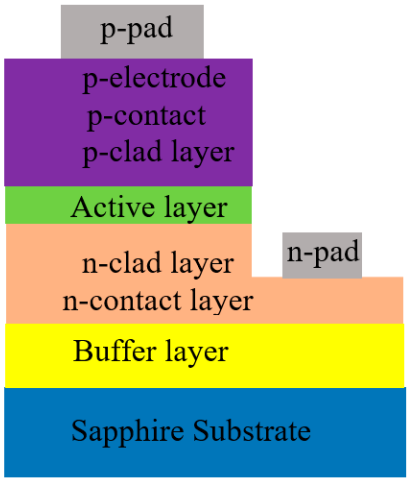


Figure 8. A basic UV-LED structure developed in 2000.

The published work by Shur et al. [66] in 2002 showed a GaN-based UV-LED with an efficiency of 0.001% at <300 nm wavelength. In 2004, its efficiency was improved to 0.01% using the alloy of gallium nitride (GaN) with aluminum, by reducing the lattice dislocation density, thereby improving the lattice mismatch issues and the crystal quality. Since then, it was only in 2009 that Hirayama et al. [67] developed AlGaN-based deep UV LEDs at 227 nm and 250 nm, with an efficiency of 0.2% and 0.43%, respectively. InAlGaN-based LEDs with a wavelength of 282 nm and an EQE of 1.2% were achieved. These LEDs were fabricated on low-threading dislocation density (TDD) AlN templates developed through a specialized ammonia (NH3) pulse-flow multilayer growth technique. The authors used MQWs, and EBL grown on the sapphire substrates, as shown in Figure 9. EBLs prevent electron leakage from the active region to the electron injector layer and also improve LED efficiency by enhancing charge separation and reducing non-radiative recombination and in turn increasing radiative recombination rates.

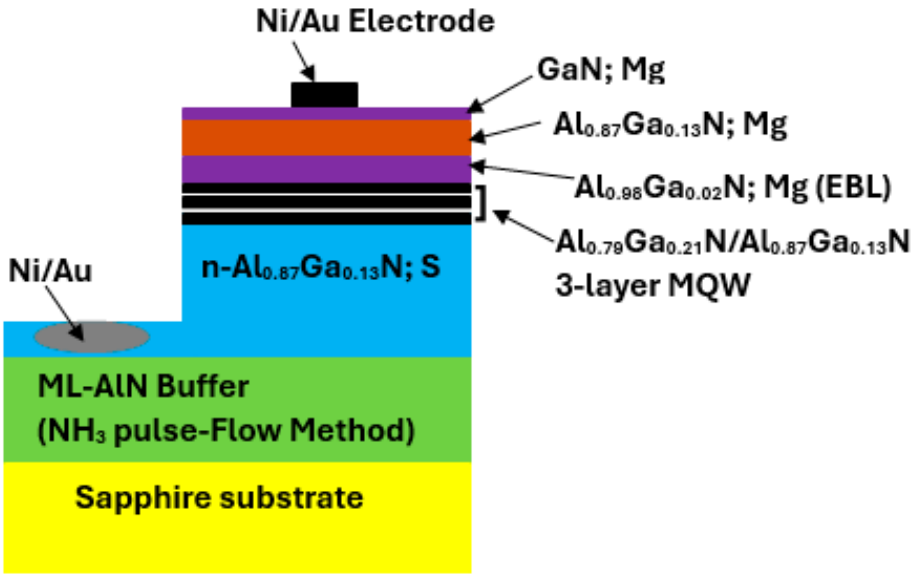


Figure 9. UV-LED structure with MQWs and electron-blocking layer for better confinement of electrons, leading to improved recombination of electrons and holes [67].

In the year 2010, Fujioka et al. were able to improve the efficiency of UV-LED of 280 nm to about 2.78%. They used multiple quantum wells in their design and high-crystal-quality AlN template optimized epitaxial structures [68]. Later in 2012, Shatalov et al. were successful in enhancing the performance of AlGaN-based deep-ultraviolet light-emitting diodes grown on sapphire substrates. The objectives were achieved by reducing threading dislocation density, improving light extraction, and optimizing chip encapsulation. With such improvements, they were able to increase the EQE to 10.4% [69]. Their findings suggest that the proposed methods have the potential to improve the performance of AlGaN-based deep-ultraviolet LEDs and may have applications in various fields.

In the year 2017, Takano et al. [70] were successful in increasing the efficiency of UV LEDs to 20.3% at 275 nm using a transparent AlGaN:Mg contact layer. They also incorporated an Rh mirror electrode, an AlN template on a patterned sapphire substrate, and encapsulation resin. The combination of the AlGaN:Mg contact layer and the Rh mirror electrode significantly improved the EQE of UV LEDs, increasing the reflection of light in the chip and eliminating absorption [70].

Later in 2018, Maeda et al. [71] developed a UV LED with 9% efficiency at 279 nm using transparent contact layers and highly reflective Ni/Al p-type electrodes. They found that when reducing the Ni layer thickness, UV reflectivity increases but the EQE decreases if it was too thin (<0.8 nm). Thus, they found an optimal Ni layer thickness of ~0.9 nm for maximum efficiency.

Further, in 2020, Pandey et al. [72] presented a detailed investigation of the epitaxy and characterization of LEDs operating at around 265 nm and found the EQE to be 11%. To achieve this, they used an AlGaN/GaN/AlGaN tunnel junction structure by incorporating a thin GaN layer between p+ and n+-AlGaN to reduce the tunneling barrier. Figure 10 is a schematic illustration of the tunnel junction LED structure.

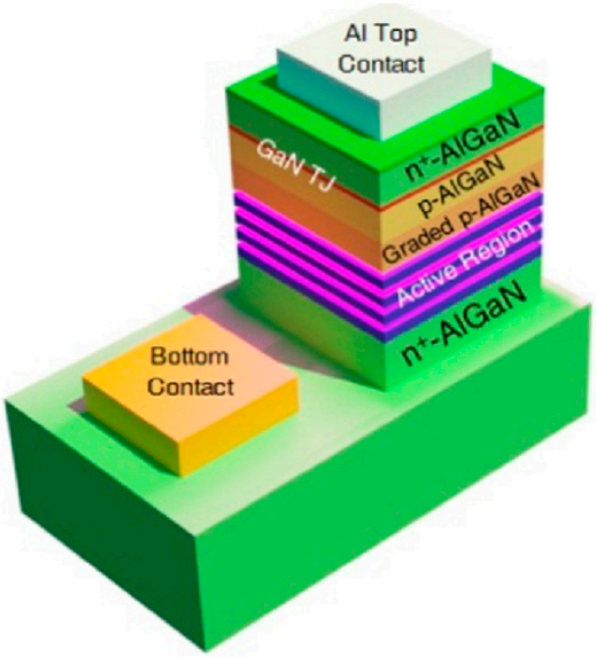


Figure 10. Tunnel junction LED structure [72].

Another recent study in 2021 by Zheng et al. [73] showed an EQE of 5.19% at 273 nm. It was demonstrated by designing a double-layer nano-patterned array for AlGaN-based deep UV-LEDs. That significantly improved light extraction efficiency. Double nano-patterned arrays on a UV LED surface act as a diffraction grating, reducing light absorption and boosting UV light output efficiency.

Designing efficient UV LEDs is indeed a challenging task that requires overcoming several obstacles to optimize device operation. The high Al composition needed in AlGaN

epilayers results in a higher TDD, causing non-radiative recombination and thereby reducing the device efficiency [74]. The low hole concentration due to the large activation energy of Mg in a high-Al-composition AlGaN alloy also results in a high-resistance p-type layer, affecting device efficiency [33]. Realizing ohmic contact in p-AlGaN is another challenging task and affects the efficiency of UV-LEDs. Relatively low light extraction efficiency (LEE) in deep UV-LEDs is attributed to transverse magnetic mode-dominant emission from high-Al-content alloys. That in turn can reduce the light output, thus reducing device efficiency [75]. Lower "electron-hole wave function overlap" due to the strong polarization effects in high-Al-content alloys reduces the radiative recombination rate, thereby decreasing device efficiency [76]. The junction heating effects, caused by the low conductivity of AlGaN alloy, also reduce device efficiency [77].

Researchers and developers are addressing these challenges steadily by improving material quality and optimizing device design. Strategies to reduce TDD include improving the crystal quality of AlGaN (3.4 eV to 6.2 eV) [78] alloy by optimizing growth conditions. Novel device designs, such as patterned sapphire substrates or distributed Bragg reflectors, have the potential to improve LEE and device performance. Addressing these challenges shows great promise in enhancing the efficiency of UV-LEDs and expanding their range of applications [78].

2.2. Evolution of Blue LED

Developing blue LEDs in the early days posed a major hurdle for scientists and engineers. They were already able to fabricate efficient red and infrared LED, but green and blue LED remained elusive. The lack of suitable materials made generating blue light significantly challenging. However, once blue LEDs were successfully developed, they enabled the formation of white light more cost-effectively and efficiently than the previous methods. Furthermore, blue LED technology has a lasting impact on various industries, including the development of high-definition displays and the popularization of blue-ray discs through the use of blue laser technology.

In this section, the evolutionary history of blue LEDs is briefly discussed. We use the Lumen/Watt (Lm/W) to explain the efficiency of LEDs. The reason for choosing the Lm/W for efficacy is that Lumens are a measure of the perceived brightness of light by the human eye. That is based on the sensitivity of the eye to different wavelengths of visible light. However, it is not possible to calculate efficiency in Lm/W for UV since it is not visible to eyes. Thus, we discussed the efficiency of UV in percentage in the earlier section. Thus, "Efficiency" refers to the proportion of light produced by a light fixture and its source when powered on, and "Efficacy" refers to the quantity of usable light generated by a source relative to the amount of electrical energy consumed, measured in Lm/W.

Increasing the current injection in LEDs leads to an increase in the amount of light output. In turn, it also increases the amount of heat generated in the LEDs. The heat can reduce the efficiency of the LEDs and shorten their lifespan. Therefore, increasing the current beyond the recommended operating range can lead to decreased efficiency and efficacy. Thus, in general, the optimum current for LEDs is the one that provides the desired level of brightness while staying within the recommended operating range to maintain the efficiency, efficacy, and life of the devices.

Figure 11 is the graph displaying the time evolution of blue LED with respect to luminous efficacy. The first blue LED was demonstrated in 1977 by Matsunami et al. [24] based on silicon carbide (SiC with Eg = 3 eV) and had an efficiency of around 0.001 Lm/W. Those LEDs were fabricated using LPE, forming *pn*-junctions by immersing a SiC substrate in a silicon melt with nitrogen as a donor and aluminum as an acceptor. However, due to SiC's indirect bandgap and low radiative recombination rates coupled with phonon-related energy losses, it was suboptimal for UV-LED applications.

The researchers were aware of the benefit of direct bandgap material over indirect bandgap material. The quest for an efficient direct bandgap material for blue LEDs had started in the early 1970's. Some of the earlier direct bandgap materials considered included

ZnSe (2.7 eV) [79] and GaN (3.4 eV) [80]. However, the realization of the efficient blue LEDs was unsuccessful. Later, in 1989, Shuji Nakamura achieved a significant breakthrough in the field of blue LED technology by developing high-brightness GaN LEDs. The resulting blue LEDs had a luminous efficacy of 2.7 Lm/W, which was a major improvement over previous blue LED efficacy [81,82]. Along with Isamu Akasaki and Hiroshi Amano, Shuji Nakamura was awarded Nobel Prize in Physics in 2014. The key contributions of these three noble laureates for efficient blue LED fabrication are shown in Figure 12.

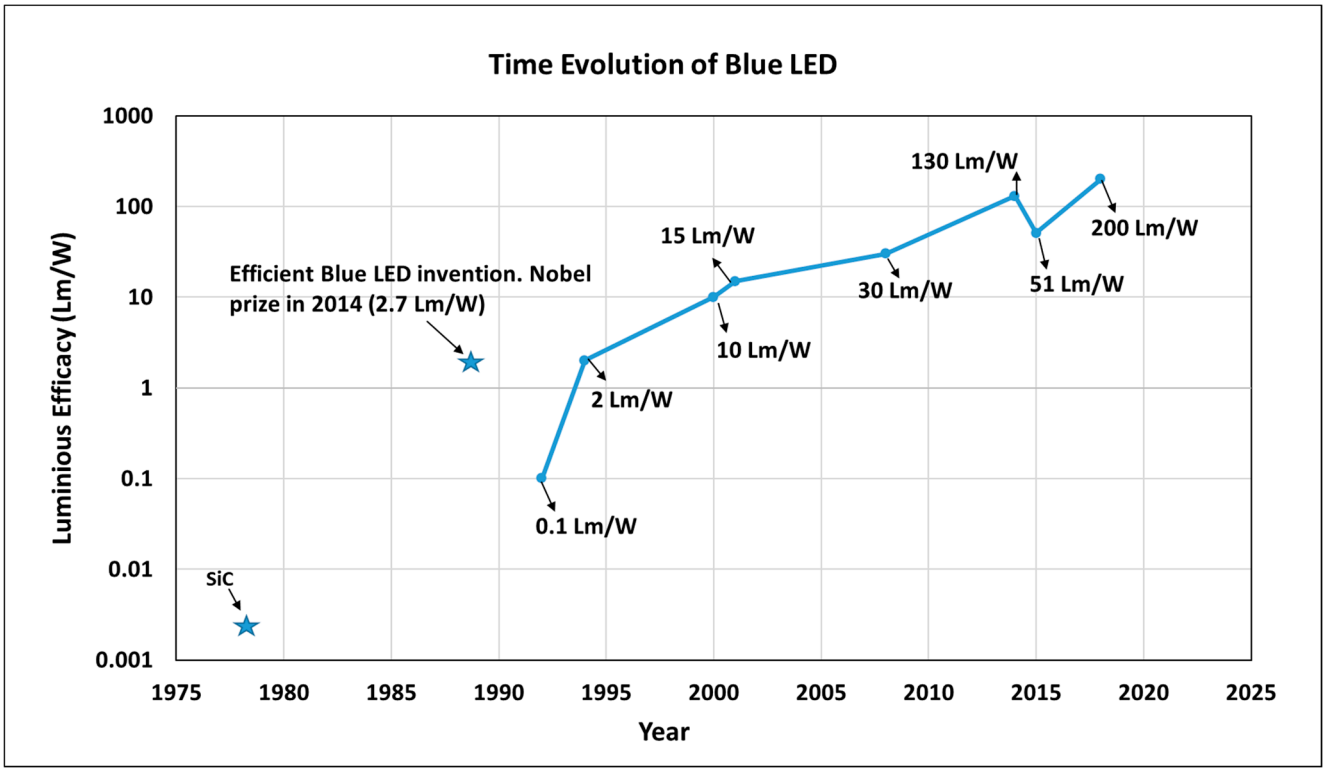


Figure 11. A graph displaying the time evolution of blue LED with respect to luminous efficacy [24,66,82–85].

According to Craford et al. [83], the efficiency of ZnSe-based blue LEDs in 1992 was 0.1 Lm/W. During that time, the low cohesive energy and poor crystallinity in ZnSe material made it less efficient. This efficiency was improved to 2 Lm/W in 1994. The improvement in material quality, p-type doping, and the epitaxial growth method were the foremost causes for the efficiency improvements.

As the exploration for improving the efficacy was going on, Shur et al. [66] showed that the blue LED efficacy reached 10 Lm/W and was further improved to 15 Lm/W in 2001. This improvement in efficiency was realized by improving the techniques for growing and processing GaN crystals. Moreover, it was attributed to new methods of doping and annealing the material to optimize its electrical and optical properties. Later in 2008, Craford et al. showed that the efficiency of blue LED increased to 30 Lm/W by improving the GaN epilayers, doping concentrations, and defect densities [83].

According to Brahmbhatt et al. [84] the efficiency of blue LED reached 130 Lm/W in 2014, improving the crystal growth quality. Optimizing the *pn*-junction (by enhanced p-type doping, optimizing thickness, adding MQWs, and improving the contact design) led to significant success.

As the research was ongoing, the work in 2015 by Krames et al. showed that the improvement in chip design, packaging, and high-current-performance blue LED increased the efficiency to 51 Lm/W [85]. According to Brahmbhatt et al. [84] the efficiency was increased to 200 Lm/W in 2018, with improvements in the quality of substrate mate-

rials, epitaxial growth techniques for internal quantum efficiency (IQE), and improved doping techniques.

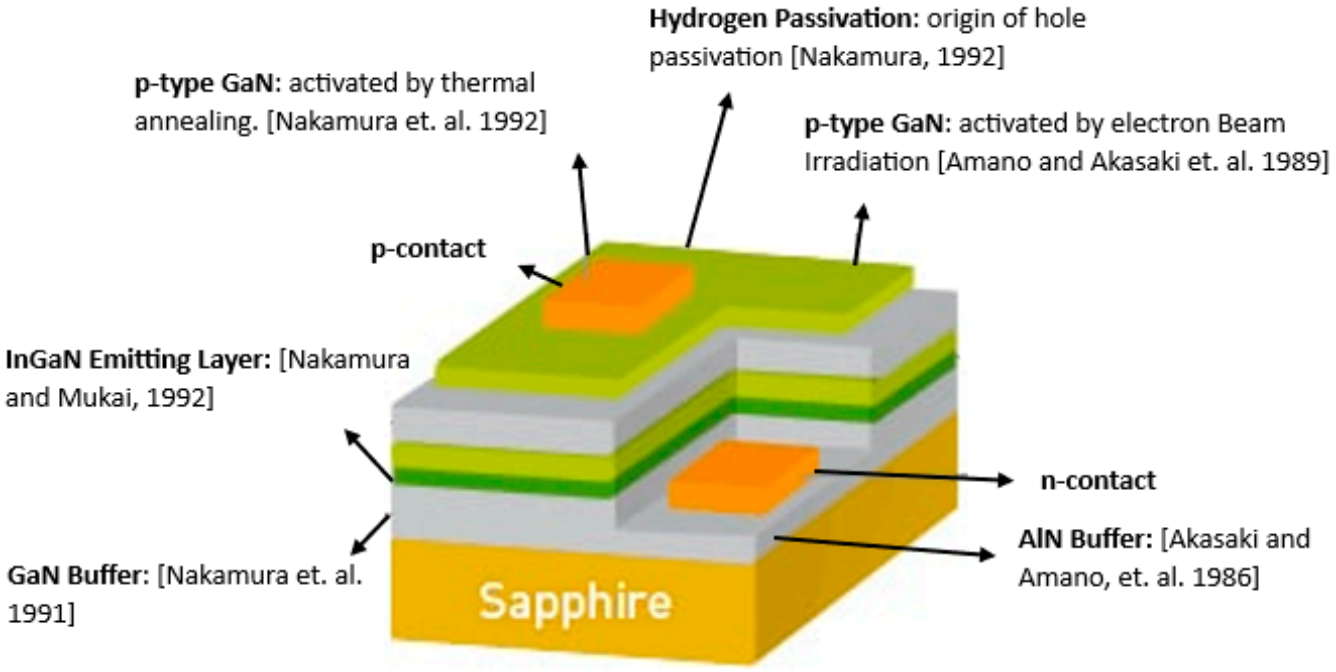


Figure 12. Figure showing the contribution of three Nobel laureates (Akasaki, Amano, and Nakamura) in producing an efficient blue LED [86–91].

Currently, the efficiency of blue LED has reached a peak EQE of 82% at room temperature and a hot/cold factor (HCF) of 94%, which has been demonstrated using the functional thin AlGaN interlayers in the MQWs [92]. Since higher efficiency (%) means higher efficacy (Lm/W), the efficacy for blue LEDs also keeps on improving as time goes on.

Extensive research is ongoing on improving the efficiency of blue LEDs, with particular attention to addressing challenges associated with chloride-based perovskites, known for their poor quality [93]. Despite these hurdles, record efficiencies have been achieved for blue-emitting perovskite nanocrystal LEDs, reaching maximum external quantum efficiencies (EQEs) of 2.4% and 6.2% at wavelengths of 465 nm and 487 nm, respectively [94]. These advancements underscore the ongoing endeavors to enhance the efficacy of blue LEDs through improvements in perovskite nanocrystal LEDs and semipolar LED technologies.

2.3. Evolution of Green LED

Historically, the first green LED was built and patented by Egon Loebner in 1958 [95]. They used lead antimonide dot alloyed to *p*-type Ge for its fabrication. There was not much research on these LEDs until the early 1970s. In the 1960s, Nicholas Holonyak Jr. was working on GaAsP materials, specifically on GaAs and GaAsP (with varying As/P ratios) substrates, as a means of making tunnel diodes. Those efforts led to the development of hetero-junction semiconductor devices, marking a significant step forward in the field. It was only in 1967 that Craford et al. [96] were able to invent the green LED using GaAsP on a GaA substrate. However, the luminous efficacy of this LED was extremely low. Figure 13 shows the time evolution of the green LED family.

In the year 1972, Akasaki et al. [97] were able to fabricate a GaP:N-based green LED with efficacy of 1 Lm/W. They used the method of LPE for its fabrication. In order to fabricate the n-side of the junction, they used sulfur instead of other donor impurities.

Though continuous research was going on, there was not much significant progress or a breakthrough in the efficacy of the green LED. It was in the year 1992 that Craford et al. [83] were able to fabricate the efficacy of a InGaN-based green LED to 2 Lm/W by

improving doping and lattice matching. For LED-based lighting applications with red, green, and blue (RGB), both red and blue LEDs became available with moderate efficiency. But green efficient LEDs remained elusive. In the LED lighting applications, this became known as 'green-gap'. Then, of course, later 'green LEDs' technology improved in efficiency to fill the gap.

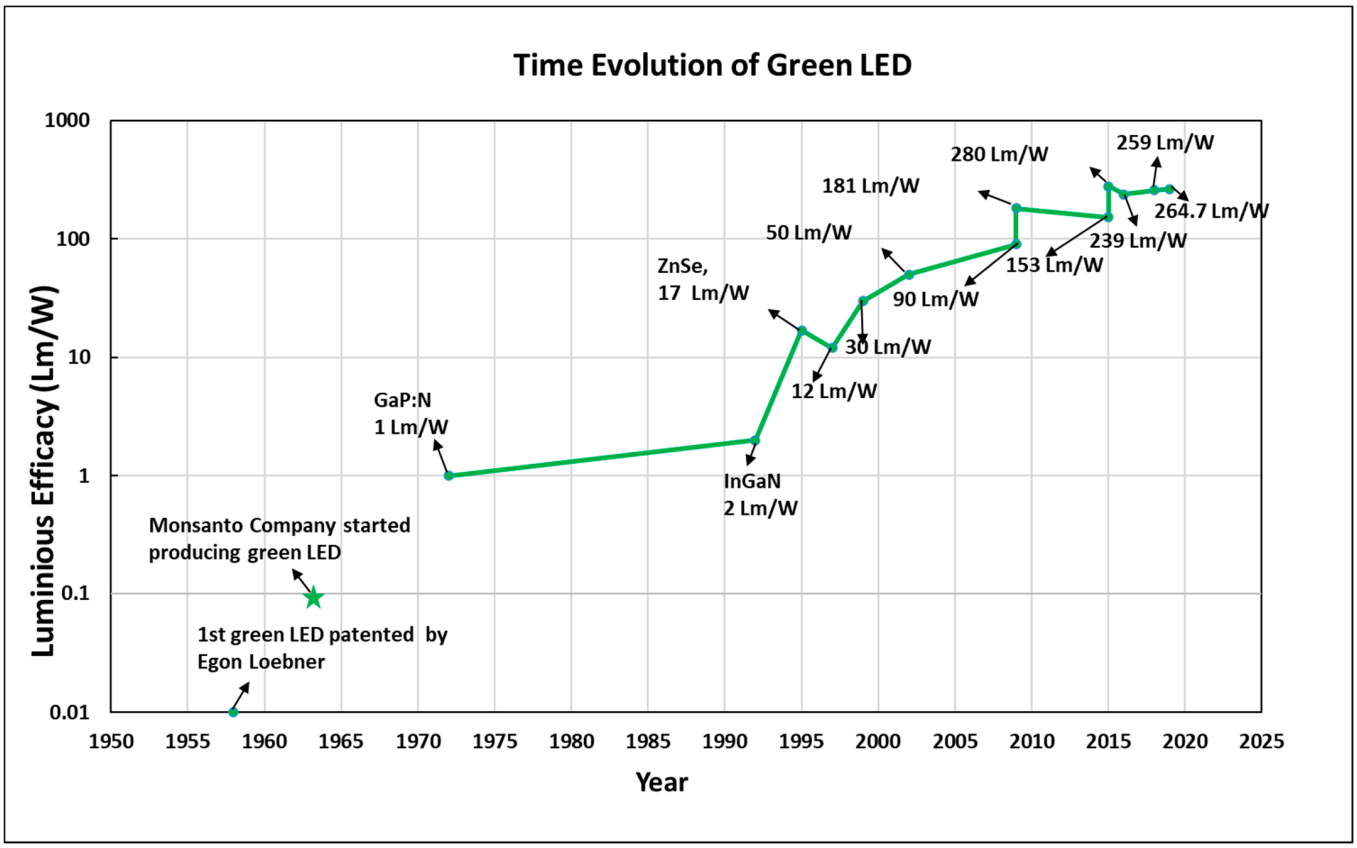


Figure 13. A graph displaying the time evolution of green LED with respect to luminous efficacy [83,95–105].

In the year 1995, another research group, Eason et al. [98], was able to fabricate a green LED with an efficacy of 12 Lm/W using a II-VI DH structure device made of ZnSe-based material. They used MBE as the method of fabrication. It was the highest efficacy for a green LED ever reported at that time. Figure 14 shows a sketch of their LED structure.

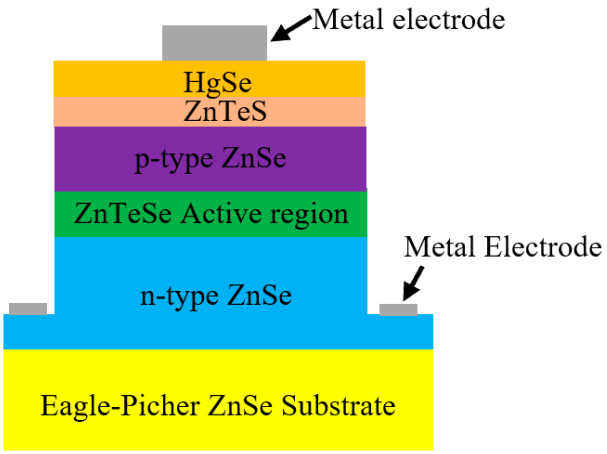


Figure 14. DH green LED structure based on ZnSe.

Similarly, in 1997, Nakamura et al. [99] used an InGaN-based material to produce an efficacy of 12 LM/W with a single quantum well (SQW). By introducing an SQW into the active region of an LED, the probability of radiative recombination was increased due to the quantum confinement effect. In SQW, the thickness of the active region was reduced to the order of the de Broglie wavelength of the carriers, leading to a quantization of the energy levels. Additionally, the use of an SQW can also lead to a narrower spectral linewidth and improved temperature stability of an LED. Figure 15 shows the design of their SQW green LED.

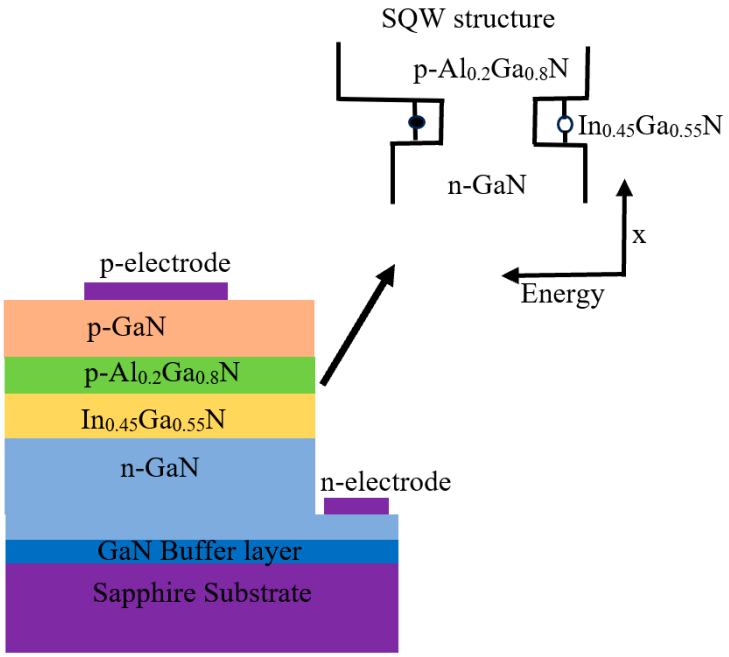


Figure 15. The structure of green SQW LED.

By the year 1999, Craford et al. [83] were able to improve the efficiency of the green LED to 30 LM/W, and by the year 2002 efficacy was improved to 50 Lm/W using the InGaN material. They were able to achieve this increased efficacy by improving the p-type doping, reducing the lattice mismatch issue and material quality. They used the superlattice structure and introduced MQWs into their design. Improvement in these factors increases the radiative recombination rate and thereby increases the light output/efficacy.

In the year 2009, Peter et al. [100], fabricated an InGaN-based green LED with four MQWs using MOVPE, with it having an efficacy of 90 Lm/W. The emission wavelength was 525 nm, and the size of the fabricated LED was 1×1 mm^2. One of the main causes of loss in InGaN based LEDs is an indirect Auger effect, which was reduced by decreasing the carrier density per emitting well and using the optimized MQWs. In the same year, in 2009 researchers from 3M Company claimed that they were able to fabricate GaN-based green LEDs with an efficacy of 181 Lm/W [101]. Instead of using a green GaN-based chip, 3M technology employed a different approach. They bonded a substance to a GaN-based blue LED chip that converts blue color to green. The material, developed by 3M, has the ability to absorb the blue light produced by the LED and emit it again as green light.

In 2015, another group, Yan et al. [102], showed the efficacy of a green LED to be 153 Lm/W. It was a GaN/InGaN based LED. They developed a strain relaxation buffer layer for a GaN/InGaN green MQW by simultaneously achieving a strain-reduced and balanced status for QWs and Quantum Barriers (QBs) in the MQW. The peak emission efficacy for their designed LEDs was 280 Lm/W. The QBs helped to confine the electrons and holes within the active region, preventing them from escaping to other parts of the device, where they would have been lost as heat. Such confinement increases the probability that the electrons and holes will recombine radiatively within the active region and emit light.

In the year 2016, Abdullah et al. [103] demonstrated very-high-luminous-efficacy green light-emitting diodes employing a $Al_{0.3}Ga_{0.7}N$ cap layer grown on patterned sapphire substrates (PSS) by MOCVD. The peak external quantum efficiency and luminous efficacies were 44.3% and 239 Lm/w, respectively. The patterned sapphire substrate interface between the semiconductor layer and the sapphire substrate can cause light to be trapped and reflected back into the device, reducing the overall efficiency of the LED. A PSS solves that problem by creating a series of small, pyramid-shaped structures on the surface of the sapphire substrate. These structures scatter and redirect the light that is emitted within the LEDs, allowing more of it to escape, and increasing the overall light extraction efficiency of the device. Figure 16 shows the schematic of their design.

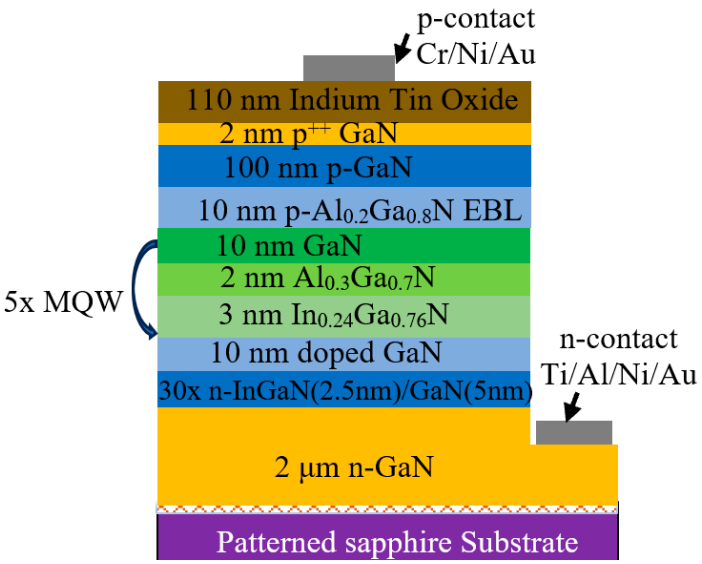


Figure 16. Cross-sectional schematic of the green LED structure.

As a continuous effort to improve the efficacy, another study in 2018 by Li et al. [104] showed that green LED efficacy was 259 Lm/W using an InGaN-based material. They used PSS, and material growth was improved using MOCVD. The crystal quality of the InGaN/GaN MQWs was assessed using X-ray diffraction; the material had few defects, and the crystal quality was significantly improved.

The next year, in 2019, Hu et al. [105] fabricated green LEDs with an efficacy of 264.7 Lm/W using MOCVD. They used an InGaN/GaN quasi-superlattice interlayer while an Al-doped Indium Tin Oxide (ITO) current spreading film was used. A basic outline of their design is shown in Figure 17.

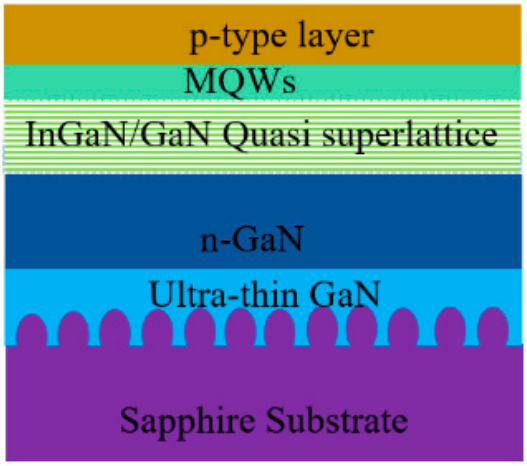


Figure 17. Schematic drawing of green LED epitaxial wafers.

Generally, green LED efficacy is lower compared to other colors (red and blue). This phenomenon, as mentioned earlier, is known in the literature as the "green gap". The green gap is characterized by a dip in the luminous efficacy of LEDs in the green spectral range of approximately 500 to 570 nanometers. This can be attributed to the poor crystal quality of 'InGaN' material as compared to GaN and AlGaN. The major source of such disparity is the lattice constants of InGaN [106]. Additionally, the green LED structure typically has a thicker active layer, which can lead to higher carrier scattering and re-absorption, reducing light extraction efficiency. Efforts are being made to address the "green gap" through advances in materials science, device engineering, and manufacturing techniques, with the aim of improving the performance and efficiency of green LEDs.

With researchers working on increasing efficiency, in 2021, InGaN-based LEDs in the blue–green light range were successfully commercialized, signifying significant advancements in efficiency [107]. In 2022, the development of pure-colored red, green, and blue quantum dot light-emitting diodes using emitting layers composed of cadmium-free quantum dots and organic electron-transporting materials were reported, demonstrating advancements in achieving high color purity in green LEDs [108].

2.4. Evolution of Red LEDs

Figure 18 is a graph displaying the time evolution of red LEDs with respect to luminous efficacy. The first practical red light-emitting diode (LED) was developed by a team of researchers led by Nick Holonyak Jr. at General Electric (GE) in 1962 [109]. They used $Ga(As_{1-x}P_x)$ for the fabrication of diodes with a polished active area of 10^{-3} cm^2 and a donor impurity concentration greater than 10^{18} cm^{-3}. Those LEDs were fabricated using vapor-phase epitaxy and emitted light at around 650 nm, with a performance of less than 0.1 Lm/W.

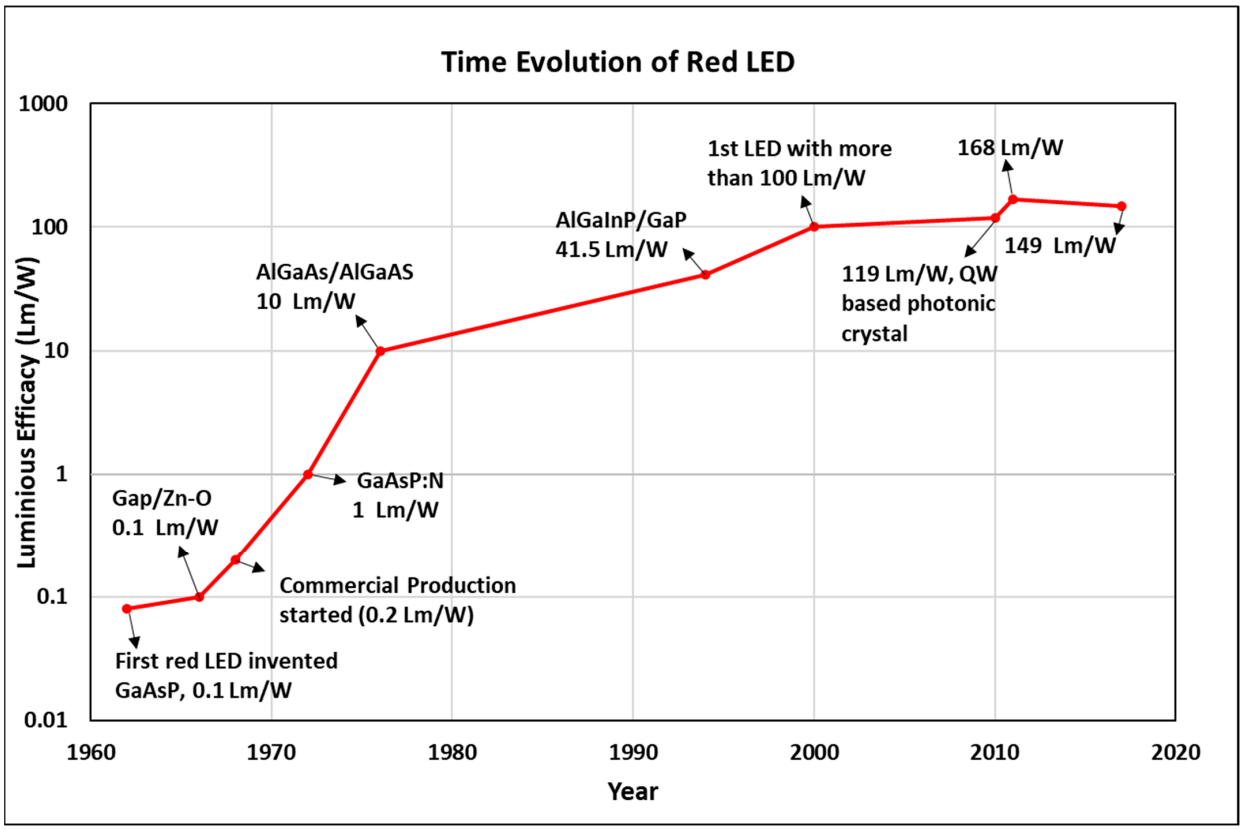


Figure 18. A graph displaying the time evolution of red LEDs with respect to luminous efficacy [83,109–115].

In 1966, Gershenzon et al. from Bell Telephone Laboratories were able to fabricate a red LED using GaP/Zn-O, with an efficiency of about 0.1 Lm/W (η = 0.007%) [110]. They found that the efficiency is determined by the relative abundance of radiative recombination centers and by the effectiveness of nonradiative recombination mechanisms. This shows that the p-type layer must contain a large number of ZnO pairs, and the crystal imperfections and undesired dopants must be eliminated from p-n junction to reduce the nonradiative recombination rate.

Later, in 1968, Monsanto Co. in Japan made a significant contribution to the field of solid-state lighting (SSL) by becoming the first company to commercially produce visible red LEDs based on a GaAsP p–n single SH junction grown on GaAs substrates [111]. The efficacy of these LEDs was about 0.2 Lm/W. Before that, visible and infrared LEDs were not widely used due to their high cost (around $200 per unit), but the low-cost production of GaAsP-based LEDs initiated the replacement of incandescent and neon indicator lamps with LEDs in various applications. Later, in 1972, Monsanto Co. was able to improve the efficacy of red LED by 10 times to 1 Lm/W by using nitrogen-doped GaAsP (GaAsP: N) [83]. Figure 19 shows the first red LED as a packaged device.

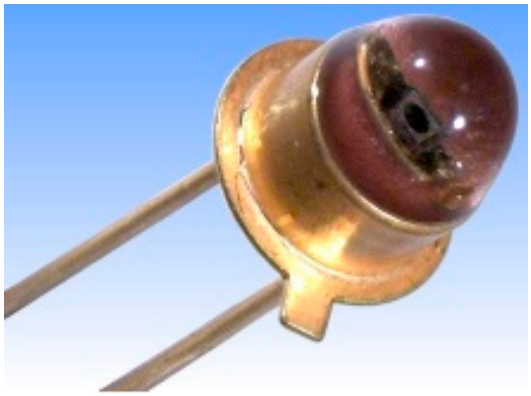


Figure 19. Monsanto MV1—the first successful red LED (http://www.lamptech.co.uk/Spec%20Sheets/LED%20Monsanto%20MV1.htm, accessed on 20 March 2024).

Until 1975, the specific defects that limit efficiency and the techniques to eliminate such defects were not studied intensively. Low efficiency, material quality, color quality, heat dissipation, and cost were the main challenges during those times [116]. The external quantum efficiency of GaP LEDs degraded under forward-biased operation. One of the causes of such degradation was the use of impurity materials such as copper. The life and efficiency of junctions grown through the LPE process were improved by ensuring that metallic impurities were removed during both the material growth and device processing stages, using high-purity gallium as the material [117].

The quest for improving the efficacy of LEDs was continuously growing. Thus, in around 1976, 'Stanley Electric Company' in Japan made significant progress in the development of high-performance red-light emitters. They used a temperature difference LPE growth technology, which was pioneered by Prof. Nishizawa at Tohoku University. The company first introduced single-heterostructure devices and then double-heterostructure devices, achieving luminous efficacy as high as 10 Lm/W [83]. This technology became a major milestone in the field of red-light emitters. Those LEDs were important because, for the first time, LEDs were bright enough to be used for outdoor applications. However, the AlGaAs layer had reliability problems in hot and humid outdoor applications.

Thus, further improvements were necessary for commercial production and applications. In the year 1994, Kish et al. [112] designed a very high-efficiency semiconductor wafer-bonded transparent-substrate (TS) using AlGaInP/GaP. A maximum luminous efficacy of 41.5 Lm/W was realized at λ∼604 nm. Thus, by the year 2000, by improving the material quality and fabrication method, Craford et al. [83] were able to fabricate a red LED based on MOCVD growth of an efficacy of more than 100 Lm/W.

Later in 2010 "Osram Opto Semiconductors R&D Lab" was able to build red LEDs using a QW-based photonic crystal that reached an efficiency as 119 Lm/W or 44% [113]. Further, in 2011, the efficiency was improved to about 168 Lm/W by improvements in chip design and material quality [114].

In 2017, Pattison et al. were able to increase the efficacy of red LEDs to 149 Lm/W [115]. Red LEDs based on 'aluminum indium gallium phosphide' (AlInGaP) materials faced two challenges. Firstly, their efficiencies decreased as the red wavelengths became shorter, and secondly, these LEDs had a higher thermal efficiency droop, requiring a control system to maintain a consistent color point. These challenges were associated with an unfavorable energy band structure in the shallow red for carrier transport, confinement, and radiative carrier recombination. This was attributed to a direct-to-indirect bandgap crossover. They suggested a possible solution could be a novel variant of AlInGaP or a different material system entirely, such as InGaN.

High-efficiency LED light sources could provide a reduction in global energy consumption. If red LEDs with an efficiency greater than 250 Lm/W can be economically manufactured, it is believed that the energy consumption for general lighting in the U.S. would be reduced by more than 60% [118]. Thus, the development of high-efficiency red LEDs has been a research challenge owing to their poor external quantum efficiency, and low internal quantum efficiency caused by material defects in the epitaxial growth and device structures.

The current research trend in red LEDs focuses on micro-LEDs and mini-LEDs, but these advancements present fabrication challenges that reduce efficiency. In 2020, researchers demonstrated ultra-small (<10 μm) 632 nm red InGaN micro-LEDs with an on-wafer external quantum efficiency exceeding 0.2%, signifying progress in achieving high efficiency in mini-displays [119]. The efficiency progress of red LEDs has also been associated with advancements in material science and device engineering. In one study, they measured the enhanced internal quantum efficiency of red-emitting InGaN/InGaN quantum wells, with a value above 10% at 640 nm, indicating substantial improvements in efficiency [120]. Furthermore, they developed 621 nm wavelength InGaN-based single-quantum-well LEDs with an external quantum efficiency of 4.3% at 10.1 A/cm^2 in 2022, indicating substantial efficiency gains in red LEDs [121].

Various techniques can be used to enhance the efficiency and output of LEDs beyond adding EBL, using MQWs, lattice matching materials, high-quality substrates, etc. For instance, incorporating organometal halide perovskite emitters between larger-bandgap layers effectively confines electrons and holes for radiative recombination [122]. It was proposed that the local doping modulation in specific quantum well barriers would suppress Auger recombination rates and reduce electron leakage, thus improving LED efficiency [123]. Moreover, the integration of heterostructure quantum dots, as explored by Bae et al. [124], has been observed to mitigate Auger recombination and achieve balanced electron and hole injection, consequently enhancing LED performance. Lu et al. [125] showed that the simultaneous doping and surface passivation of perovskite nanocrystals could enhance photoluminescence quantum yield and stability, leading to improved LED performance. These techniques, along with interfacial control, charge transport enhancement, and geometrical optimization, collectively contribute to advancing LED efficiency and output capabilities.

Now, in the upcoming sections, we will focus on the different applications of LEDs. LEDs are widely used in various fields due to their diverse applications and advantages. The key parameters that indicate the performance of LEDs in different applications include internal quantum efficiency, extraction efficiency, drive current, operating temperature, and optical coupling efficiency [126]. These parameters are crucial for high-luminance applications and enable higher lumen/USD ratios. LED applications span across fields such as lighting, indicators and displays, farming, medicine, and communication [111]. The development in packing and coating technology has led to a decrease in the size and cost of LEDs, making them suitable for applications such as street lighting, digital boards,

sign boards, architectural buildings, and automotive lighting [127]. Additionally, wearable LED patches are being investigated for photo-medical applications such as dermatological treatment, alopecia, and Alzheimer's disease treatment, owing to their noninvasive, portable, and safe use [128].

In the field of optoelectronics, LEDs have been integrated with chemical/pressure sensors and off-chip communications circuitry, demonstrating their versatility and potential for directed cell growth or remediation [129]. Furthermore, quantum dot light-emitting devices (QLEDs) have shown promise for various photo-medical applications, including cancer cell treatment and cell metabolism enhancement [130]. However, it is noted that current OLEDs or QLEDs may not be suitable for applications requiring strong light, such as photodynamic therapy [131]. Thus, LEDs exhibit a wide range of parameter indicators that are crucial for their performance in various fields, including optoelectronics, bioimaging, photo-medical applications, and communication. The diverse applications of LEDs underscore their significance in modern technology and their potential to address multifaceted challenges across different domains.

3. Prospects of LED Lighting Technology

3.1. Application of LED in White Lighting

Generally, white light can be produced from three mechanisms. One method is by mixing the three primary color LEDs, red, green, and blue (RGB), in appropriate proportions. Thus, after the invention and optimization of blue LEDs, white light was successfully obtained by mixing these three primary colors. The other method of producing LED-based white light is use of the "phosphor method". This allows the production of white light by single-color LEDs using short-wavelength LEDs such as UV or deep blue with a yellow phosphor coating [132,133]. However, a third method for white light production is by the combination of RGB phosphor with UV. Figure 20 is the pictorial representation of the production of white light using the three different methods.

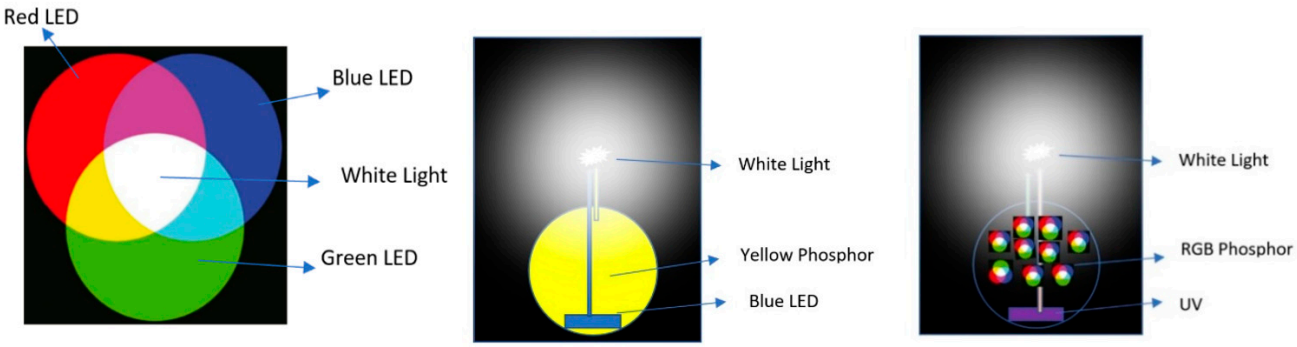


Figure 20. White light can be produced using red, green, and blue LEDs (**Left**); white light can be produced from blue LED and yellow phosphor (**Middle**); and white light can be produced from RGB phosphor and UV light (**Right**).

After the discovery of methods for producing white light using blue LEDs, there has been significant development in SSL in the past decade. White light-based LED technology was developed in Japan in 1972 and its basic structure consisted of an LED Chip and fluorescent element used in solid-state lighting systems [134]. LED lighting technology is the fourth and latest generation of light sources after incandescent, fluorescent, and HDI lamps, respectively. Improvements in efficiency and cost reduction were the leading cause of the monumental paradigm shift.

LED technology readily surpasses the benefits of other conventional light sources in terms of lifespan, compactness, portability, efficiency, zero toxicity (no mercury contents), and a negligible IR and UV content. Moreover, LED-based lighting renders itself for selected spectral contents, architectural appeal and ease, and biochemical and desired biophysical effects.

In order to generate white light from LEDs that is comparable to natural light, there must be an optimal color rendering. If the color of the light is not equivalent to sunlight or light from a filament bulb, it will be different from the natural one and can cause some difficulties in the eyes [135]. Recent advancements in III-Nitride materials in semiconductor technology have revolutionized SSL and LED technology, emphasizing the need for highly efficient and durable materials. The basic principle involves injecting electrons into the conduction band, leading to recombination with holes in the valence band and the production of photons with energy matching the semiconductor's bandgap.

The recent developments in the SSL are also focused on energy saving and environmental friendliness. Due to the SSL device's vibrant and shock-resistant nature, various design possibilities [136], intensity, and color availability, these lights have a wide range of applications from home to street lighting, and decorative and environmental effects. A compound annual growth rate (CAGR) of 10.5% is forecasted for the LED lighting market from 2022 to 2030, valuing it at USD ~60 billion in 2022 and 133 billion in 2030 [137]. The main reason behind such growth is that workplace lighting must meet/comply with the government's standards and regulations for low energy consumption and efficient lighting devices. Figure 21 shows the growth in the North America LED lighting markets.

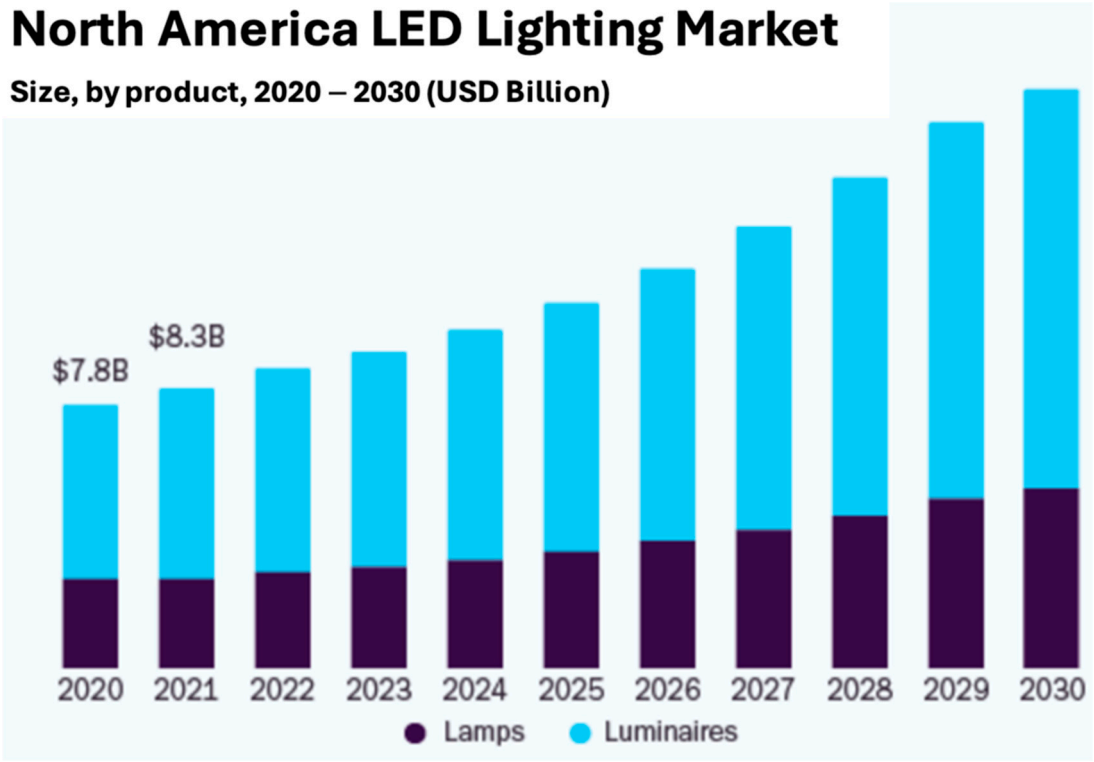


Figure 21. North America LED lighting market predicted from 2020 to 2030 [137].

In addition to the semiconductor-based material discussed in the foregoing pages, LEDs can be fabricated from organic materials as well. Here, we briefly review and discussing various lighting techniques and their applications in architecture, agriculture, entertainment, and therapy.

3.2. OLED Lighting

OLEDs stands for Organic Light-Emitting Diodes. This technology can be used for lighting applications because of its ultra-thin, lightweight, and homogeneous light emission nature. OLED technology can readily be used to create SSL by sandwiching thin, carbon-based organic layers between two electrodes [138]. Organic molecules are excited when DC bias is applied for injecting holes from the anode or electrons from the cathode, respectively.

The wavelength of the light produced depends on the structure of the organic molecule used. Figure 22 shows the basic principle of the devices used in OLED lighting.

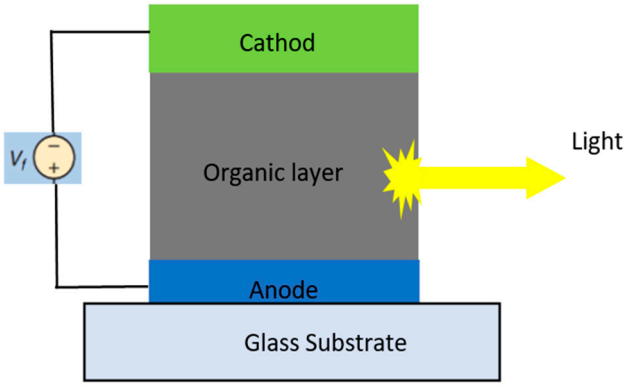


Figure 22. A typical structure of an OLED.

OLED light bulbs offer enhanced flexibility and customization, making them a popular alternative for homes and businesses. Unlike LEDs, OLEDs use stacked organic material on a glass or plastic substrate, while LEDs grow inorganic layers on various substrates. OLEDs provide soft, diffuse illumination, contrasting with the concentrated light of LEDs, which often require additional optical apparatuses. LEDs are primarily used for residential, commercial, and street lighting, whereas OLEDs are designed for energy-efficient interior, decorative, and mood-enhancing lighting.

Organic materials lie at the core of OLED technology, crucial for light emission, charge transportation, and device reliability. Small-molecule organic compounds, characterized by a low molecular weight and precise chemical structures, form the foundation of OLEDs, commonly deposited as thin films through methods like vacuum thermal evaporation. The materials used in making OLEDs primarily consist of organic compounds, including polymers, small molecules, and fluorescent or phosphorescent materials [139]. These materials are known for their flexibility, low cost, and easily controlled preparation, making them ideal for OLEDs. The third generation of emissive materials for OLEDs includes thermally activated delayed fluorescent (TADF) emitters, which have become the leading emissive materials for highly efficient OLEDs [140]. Additionally, blue fluorescent materials, especially deep-blue fluorescent materials, are indispensable in OLEDs due to the relatively poor stability of blue phosphorescent materials [141]. Furthermore, the use of thiophene-based materials has shown improved optical performance in OLEDs due to their outstanding chemical and physical properties [142]. Thus, the materials used in OLEDs encompass a wide range of organic compounds, each contributing to the unique properties and performance of OLED devices.

3.3. LED Lighting in Agriculture

It has been widely researched, established, and accepted that LED lighting (with selected wavelengths/colors) can significantly improve productivity in plants. The intensity, duration, and spectral properties of the lighting are critical factors in determining the extent and character of plants' growth and development [143]. Research at the University of Wisconsin showed that a combination of red LEDs and blue fluorescent lamps could elongate the hypocotyls and cotyledons of lettuce seedlings [144]. However, this effect could be prevented by replacing blue light with 15 $mmolm^{-2}S^{-1}$ [145]. Red light has shown impacts on the flowering and promoting internode elongations of plants [146,147]. Blue light showed its impact and importance in phototropism and stomatal opening [148,149]. These findings suggest that LED applications in agriculture could alleviate future food scarcity. Efficient LEDs may revolutionize crop productivity and the lighting color combination can lead to multiple crops in short period harvesting. Tailored lighting algorithms based on plant responses could enhance yield, quality, and efficiency, reducing costs and time cycles.

3.4. LED Lighting in Decoration and Entertainment

LED lighting products are widely being used in numerous entertainment and decorative applications. These include various events, concerts, stage, home, automobile applications, and much more. Owing to the availability of a wide variety of colored LEDs that can even be used as enhancements to artwork, LED lights themselves are being used as artwork and are environmentally friendly. Special events are yet another place where LEDs and LED lighting products find perfect usage. Party planners, event planners, caterers, DJs, audio/visual specialists, and other special event planners or designers use LED lights to add accents, single-color ambient lighting, or even color changing RGB LED lights to jazz up their parties or events.

3.5. LED Lighting in Therapy

Various experiments have shown that LED light has its therapeutic effects. LEDs are used for a wide range of medical conditions through phototherapy. According to dermatological trials, LEDs treat acne vulgaris, wound healing, skin rejuvenation, photoaging, and inflammatory conditions safely and effectively. Red LED (670 nm) daily irradiation reduced oral mucositis severity and incidence among pediatric patients [150]. There is a growing trend among people seeking solutions such as photo-rejuvenation to treat aging skin conditions including sun damage, hyperpigmentation, and enlarged pores. For this, LED therapy can be a potential antiaging technique [151]. Yellow LED lighting with wavelengths between 570 nm and 590 nm can penetrate the skin up to 2 mm depth. As an adjuvant treatment after laser therapy, Yellow LEDs have been used to treat stress and photo-aging. The adjuvant effect of Yellow LEDs is seen in patients who receive intense pulsed light. According to a blind observer, the erythema and pain on the irradiated side were reduced by approximately 10% [152]. It has been reported in many studies that blue light is effective in treating Gram-positive bacteria such as P. acnes [153]. Actinic keratosis and acne vulgaris can be treated with blue light with a wavelength of 400–470 nm since it penetrates to a depth of 1 mm. Moreover, due to its porphyrin content, P-acne contains oxygen free radicals that promote its effect on acne in the presence of blue light. With all these discussions on the application of LEDs in therapy, it is evident that LEDs are effective in therapy and the medical field. Further research and the area of application has to be established for its maximum application.

Despite the considerable advancements in utilizing LEDs for solid-state lighting, there are still obstacles preventing the realization of their maximum benefits or output. Ensuring the stability and efficiency of LED lighting devices is crucial across various applications such as lighting, display, communication, sensing, imaging, and medical diagnostics [154]. A significant challenge lies in discovering phosphors with high quantum efficiency, improved thermal stability, and controllable excitation/emission properties to enhance the performance and versatility of LED lighting systems [155]. Additionally, urgent efforts are needed to develop flexible LED components that can meet the diverse demands of modern lighting applications, where flexibility and adaptability are essential requirements [156].

4. Applications of LEDs in Display Technology

Contemporary electronic devices are inextricably linked to pervasive display technology. The displays in electronic devices have enormous applications in smartphones, tablets, computers, laptops, TVs, projectors, and VR/AR devices. In the advertising industry, large-size display screens require improvement for cheaper and more efficient systems. Prior to the invention of the Liquid Crystal Display (LCD) system in the late 1970s, bulky and heavy cathode ray tubes (CRTs) were the dominant technology [157,158]. However, LCD technology also required backlighting units, which had limited flexibility and a large thickness. This made those display-systems bulky and complex. Owing to improvements in semiconductor materials and advancements in manufacturing techniques, there is the widespread use of LED and OLED display systems [138,159]. OLEDs are an even better

technology because of their smaller thickness and better freeform factor. This technology, being self-luminous, has a wider view angle, high contrast, and fast response, and is power saving [160,161]. However, it needs improvements in lifetime, efficiency, and mass production capacities.

When LEDs are used as pixel-based resolution, the size of the LED has to be reduced for high color saturation, high brightness, and power saving [162]. The High Dynamic Range (HDR) is the basis for next-generation displays. The LED display technology is being optimized in the form of OLED, mini-LED (mLEDs), and micro-LED (μLEDs) displays. In the forthcoming sub-sections, we present a brief analysis of diverse display technologies.

4.1. Liquid Crystal Displays (LCDs)

In LCD technology, there is fluorescent backlighting behind the screen to provide illumination for the colors on the screen; LCDs have an LCD panel in the front that can show colors. In recent years, LCDs have become increasingly obsolete, and production is close to ceasing. Due to the fluorescent backlighting just behind the LCD panel, these are relatively cheap but quite thick. Black does not reproduce well due to the bright backlighting, which casts a greyish shade on the black parts or the corners. Since there is only one backlight, it cannot be dimmed at one point behind the display. LCDs require a lot more energy because they are fluorescent backlit; however, they are/were better than CRT displays in terms of energy consumption.

4.2. Plasma Display

In plasma display panels (PDPs), small cells containing plasma, an ionized gas that responds to electric fields, create a display. However, low-cost LCD and high-contrast OLED flat-panel displays have reduced the market share of plasma displays to nearly zero. Market share of PDP dropped very low by 2013 and its manufacturing was stopped in the US in 2014 and also stopped in China in 2016 [163].

Compared to OLED displays, plasma displays consume a lot more power and are quite thick. Additionally, they consume a lot of power even though they do not offer a very impressive contrast ratio. Although plasma displays reproduce black colors more accurately than LCD and LED displays, they are not as good as those OLED displays.

4.3. OLED Displays

OLED displays emit visible light, not requiring backlights. They can produce deep black levels and can also be made thinner and much lighter than LCDs [164]. OLEDs typically emit less light per area than inorganic counterparts due to their low thermal conductivity. The main benefits of OLED displays are their better response time, energy efficiency, wider viewing angles, flexibility, and softness on the eyes. The disadvantages of OLEDs include their relatively shorter lifetime, sunlight effects, and highly water-prone and moisture-sensitive nature.

4.4. Mini-LED (mLED) Displays

mLED displays use LED backlighting for local dimming, with over 1000 full array local dimming zones (FALD) [165]. The mLED display is used for the backlight unit rather than a display's pixels for the LCD system, as it must have both an excellent dark state and high peak brightness to achieve a HDR with a contrast ratio (CR) greater than 100,000:1 [166,167]. The mLED size generally ranges from 100 to 200 μm. Thus, because of the smaller size, more LEDs can be used for the backlighting, which increases brightness and improves contrast.

4.5. Micro-LED (μLED) Displays

The first μLED was reported to be built in the year 2000, with a thickness of 12 μm, at Texas Tech University [168]. The μLED does not use LED backlighting for the display; however, it can control its individual pixels for better contrast. The size of the μLED is generally less than 100 μm. In order to increase the flexibility of the μLED, the flexible

substrate can be combined with the µLED [169]. According to "Research and Markets", the global µLED display technology market will increase to USD 20.5 billion by 2025, with a compound annual growth rate of about 80% [170]. It is estimated that the micro-LED display market will reach 330 million units by 2025 [171]. Figure 23 forecasts the increase in the use of different display devices with a micro-LED display.

The µLED display technology is in its early stages. In order to commercialize the µLED technology, the challenges, e.g., the transfer printing of µLED chips for commercial production and full-color method for display applications, have to be addressed [172–174].

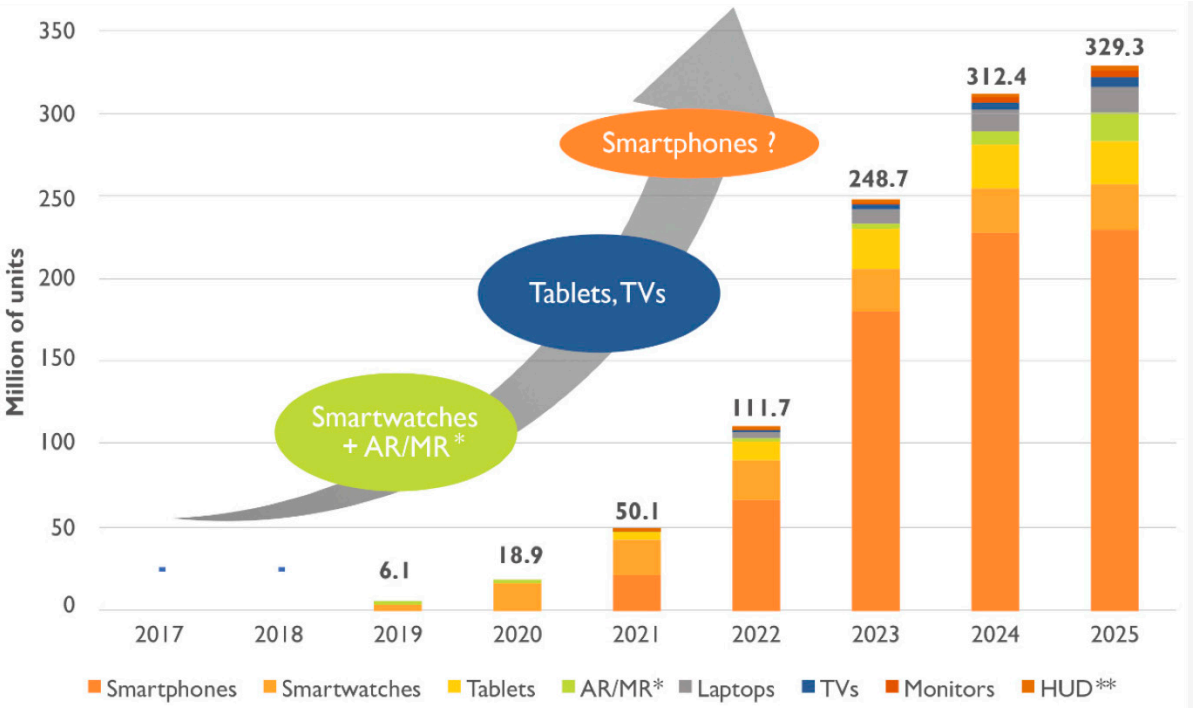


Figure 23. Forecast of development in micro-LED display [175].

It was observed that the development of color filtering and display technologies has primarily been focused on high resolution, color vibrancy, and high efficiency, as well as slim dimensions. Metallic nanostructures can manipulate the properties of light to achieve these goals through surface plasmon resonances [176].

Plasmonic colors arise from resonant interactions between light and metallic nanostructures. This promising field of research could have a significant technological impact on the engineering of plasmonic colors. Furthermore, quantum dot-based displays could also be the future of display technology. Nanoparticles with semiconductor properties called quantum dots are man-made nanoparticles. Typically, their size ranges from two to ten nanometers, and their size determines the wavelength (color) of the light they emit. Light sources based on quantum dots (QDs) emit specific colors corresponding to their bandwidth: If the dots are larger, they will emit red light, while if they are smaller, they will emit green light. Quantum dots showcase several advantages for display applications, including their high illumination efficiency, color rendering, low cost, environmentally friendly nature, and mass production capability [177].

Next-generation light-emitting diodes (LEDs) in lighting and display applications may employ these QD materials as alternative light-emissive materials. Although QLEDs have excellent performance, several factors limit their efficiency, including nonradiative recombination, energy transfer, and field-induced quenching. Moreover, the majority of past research has focused on Cd-based quantum dots, so their commercialization has also been limited. QD properties have been understood in more depth, their application in LEDs

has been explored, and challenges to making high-efficiency QDs have been overcome since the development of nanotechnology [178].

With all these discussions and reviews on display technologies, it is difficult to predict which display technology will win in terms of mass production and utilities in the future. However, ostensibly μLEDs and quantum dot-based display technology may surpass the other display technologies [175,178].

As discussed above, μLEDs and OLEDs are two emerging and promising technologies for display applications. Fabrication of these LEDs with higher external quantum efficiency is indispensable for their future application and economical manufacturing. Figure 24 shows the current status of the EQE of μLEDs and OLEDs for three primary colors.

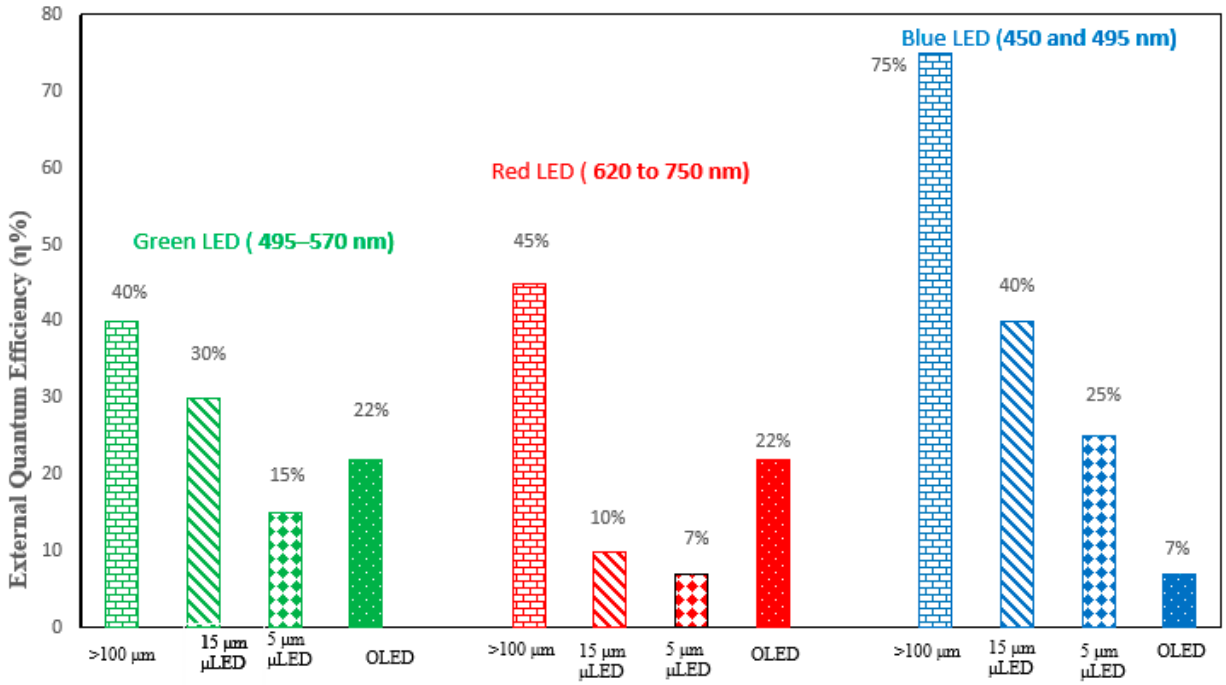


Figure 24. Improvement in external quantum efficiency of μLEDs vs. OLEDs producing three primary colors. [Graph recreated using data from Yole (https://displaydaily.com/porotech-could-be-disruptive/, accessed on 20 March 2024)].

Since then, LED technology has made substantial progress in display sectors. Specifically, the introduction of inorganic mini-LEDs (mLEDs) and micro-LEDs (μLEDs) has boosted the performance of LCDs and facilitated the creation of sunlight-readable emissive displays [179].

Despite notable advancements in LED technology, significant challenges persist in the mass transfer process for manufacturing micro-LED displays, impeding their full development [180]. Mass transfer technology aims to efficiently and accurately transfer millions or even tens of millions of Micro-LED pixels from sapphire substrates to the glass substrates needed for display devices. This process ensures proper electrical and mechanical connections between the Micro-LED pixels and the drive circuitry. LED luminous output falls short compared to traditional UHP lamps, posing a bottleneck in applications such as micro-projection displays, where brightness is crucial for image quality [181]. Thus, addressing these technical hurdles is crucial for realizing the full potential of micro-LED displays in various applications.

5. Applications of LEDs in Disinfection of Microbes

The air, water, and surfaces of various objects are often soiled with bacteria and viruses that we encounter every day. People touch these frequently, which increases their chances of getting infected. Thus, to control those harmful pathogens and their effects, UV-C exposure

has proven effective in disinfection and thereby reducing the likelihood of infection in humans and cross-contamination. Therefore, the most efficient and environmentally friendly method to disinfect surfaces and closed environments might be the use of UV-LEDs. In order to produce UV-C radiation, extra-wide-bandgap semiconductors are utilized. In the following sections, we will discuss the use of UV-C LEDs in water purification and surface disinfectant processes.

5.1. Application of UV-LEDs in Water Purification

Safe drinking water is a paramount worldwide issue, as almost 800 million people lack access to basic drinking water. Globally, at least 2 billion people use water sources that are contaminated with pathogens such as bacteria and viruses. Contaminated water is the major cause of transmittance of diseases, e.g., diarrhea, cholera, dysentery, typhoid, and polio. Drinking contaminated water is predicted to cause ~485,000 diarrheal deaths each year. By the year 2025, half of the world's population will be under water stress [WHO, June 2019] [182]. Consequently, providing safe drinking water cost-effectively using UV LED-based purification technology is very promising.

UV light exposure is one of the effective methods of disinfection and is widely used in equipment sterilization through a germicidal UVC of ~254 nm emitted by a mercury (Hg) lamp. Due to Hg's toxic nature, disposal issues, and its vulnerability to shock and vibrations, mercury-based UV lamps are being replaced by UV LEDs. UV LEDs have unique properties compared to other conventional UV sources. There is a high demand for improved disinfection applications, especially for water treatment and microbial disinfection usage. UV LEDs can be highly effective in deactivating pathogens that are chlorine-resistant and produce negligible amounts of byproducts. They are easy to retrofit into existing treatment units [183]. Water purification prototype and sterilization systems based on UV LEDs have been demonstrated using wavelengths in the 210-to-365 nm range [66,184].

Numerous studies have delved into the effectiveness of different wavelengths in deactivating bacteriophages, bacteria, and viruses. A noteworthy investigation by Cheveremont et al. [185] highlighted the potent microbial reduction achieved through the coupling of UV-A and UV-C in wastewater treatment. Furthermore, the specific combinations of 280/365 and 280/405 nm proved highly effective in significantly reducing mesophilic bacteria.

The methods used in the study involved precise analytical techniques and multiple measurements to ensure accuracy. The research aimed to assess the effectiveness of UV LED irradiation in treating wastewater and to understand its impact on various parameters such as organic carbon, nitrogen, and metal concentrations. For the exposure of 280/365 nm LED coupling, the log reduction for Mesophilic bacteria and fecal enterococci was 2.3. The log reduction for total coliforms and fecal coliforms was 3.7 and 3.2, respectively [186].

While UV-C light demonstrates remarkable efficiency in virus elimination, it faces limitations in penetrating certain cellular layers and structures, such as the outer dead cell layer, the ocular layer in the eye, and the cell cytoplasm. Encouragingly, UV-C light has been established as a safe method for eradicating a broad spectrum of viruses without causing harm to human skin [187,188].

The research of Oguma et al. [189] provided valuable insights into the inactivation of E. coli using UV LEDs at varying wavelengths. Notably, 265 nm and 280 nm UV LEDs achieved over 4 log inactivation of E. coli at dose levels of 10.8 and 13.8 mJ/cm², respectively. In contrast, the 310 nm UV LED requires a substantially higher dose level of 56.9 mJ/cm^2 for a 0.6 log inactivation.

Our investigation centered on the bacteriophages MS2 and Phi6 as these are the microbes frequently used in disinfection research. MS2 represents non-enveloped viruses, while Phi6 stands as an exemplar for enveloped viruses. Both these bacteriophages have been widely adopted as surrogates for assessing the environmental behavior of pathogenic viruses [190,191]. One of our previous studies showed that our designed 275 nm UV LED was able to deactivate the bacteriophages MS2 and Phi6 using a UV dose of 26.82 mJ/cm^2 and 32.81 mJ/cm^2, respectively. The corresponding log reduction was 1.16 and 1.26,

respectively [192]. The "inactivation-efficiency" also depends on the nature of the microorganism, wavelength dependence, and UV dose level. It was observed that diverse microorganisms have different responses to UV wavelengths. For the Escherichia virus, i.e., MS2, it can be inactivated at 280 nm with a UV dose of 30.5 mJ/cm^2. Numerous studies have suggested that UV-C LEDs are more effective in deactivating pathogens. Table 2 summarizes the dose response and log inactivation in some microbes, using UV-LED for microbial disinfection.

Table 2. Table showing wavelength, dose–response and log inactivation in some microbes (*E. coli*, MS2 and Phi6) using UV LEDs for water disinfection.

Wavelength (nm)	Microbes	Disinfection Medium	UV Dose (mJ/cm^2)	Log Inactivation	Dose Response mJ/cm^2 per log Inactivation	References
255	MS2	Water	41	3.2	12.8	[193]
255	Ms2	Water	60	2.3	26.1	[194]
255	E.Coli	Water	9	2.7	3.3	[194]
254	Ms2	Gelatin-based medium	2.51–6.5	2	1.25–3.25	[195]
254	Phi6	Gelatin-based medium	7.75–10	2	3.87–5	[195]
260	MS2	Double agar layer	30.3	2	15.15	[196]
280	MS2	Double agar layer	38.5	2	19.5	[196]
260/280	MS2	Double agar layer	32.8	2	16.4	[196]

Accordingly, from these reviews, we conclude that UV-LED would be better alternative for water treatment and pathogen inactivation compared to traditional disinfectants and other UV sources. Since UV-LEDs do not contain mercury, consequently there are no disposal problems. Due to their robust and compact nature, they are more durable and relatively easier to handle. Thus, there is great potential for improving the efficiency, cost, and lifetime of UV LEDs for future applications in diverse areas.

5.2. Application of UV LEDs in Microbial Disinfection from Surfaces

The outbreak of Coronavirus disease in December 2019 (COVID-19) caused by coronavirus 2 (SARS-CoV-2) has infected more than 704 million and resulted in the death of more than 7 million people worldwide (as of 2 May 2024) (WHO COVID-19 data). This has become a major challenge to the scientific and medical community and to the entire human civilization. Research is ongoing about the virus; however, there are no effective and well-approved methods for inactivation that have yet been developed for wide adoption. UV radiation is effective in deactivating different bacteriophages such as MS2, T4, T7, and bacteria like E. coli [197]. Consequently, there is a promise that UV LED irradiation can be effective and promising technology for SARS-CoV-2 deactivation. The size of SARS-CoV-2 is about 100 nm, with a volume of ≈106 nm^3 and a mass of ≈1 fg [198]. Figure 25 shows the general structure of a coronavirus. Coronavirus has a single-stranded, non-segmented RNA genome coated by a protein and lipid envelope. If there is any damage to these components, this could lead to the inactivation of the viruses [199]. Also, UV light employs a range of mechanisms to inflict damage on viruses and bacteria, as elucidated in Figure 26. There are major five mechanisms for microbial deactivation by UV radiation. They are thymine formation, protein cross-linking, inactivation of enzymes, oxidative damage, and disruption of the protein structure.

Thus, UV-C LEDs could be highly effective in controlling such viruses. UV-C LEDs of specific wavelengths and particular doses and a certain exposure duration could be highly effective in the sterilization of contaminated surfaces, leading to inactivation of the virus [200]. It has been observed that the UV-C light of wavelengths of 207 nm to 222 nm has been proven to be highly efficient in killing various microorganisms without causing a harmful effect on the skin [201]. The penetration ability of these wavelengths is limited

as compared to other sources of UV (254 nm) [187]. However, this limited penetration is enough to pass through the size of the virus. Thus, UV-C light efficiently kills the virus but cannot penetrate the outer dead cell skin layer, the ocular layer in the eye, or the cytoplasm of the cell. Thus far UV-C light has been proven to be safe for killing a wide range of viruses without damaging the human skin [187,188].

It is worth mentioning here that III-V AlGaN/AlN-based Quantum Well LEDs are a mature and established technology. However, achieving wavelengths below 250 nm has been challenging. Despite this, an Australian company, Silanna UV, recently reported success in developing 225 nm UV LEDs using the short period superlattice (SPSL) technique. Their approach, utilizing AlN and GaN, shows promise for high-efficiency short-wavelength UV LEDs [202,203]. Keeping in mind the length of the present review manuscript, we are only providing the references of the breakthroughs deserving a separate review paper to fully describe the physics and engineering of these far/deep-UV devices. This discovery could be one step closer to a high performance and highly efficient disinfection system. Now, the nature of microbes (coronavirus) and the response of microorganisms to UV radiation is analyzed further.

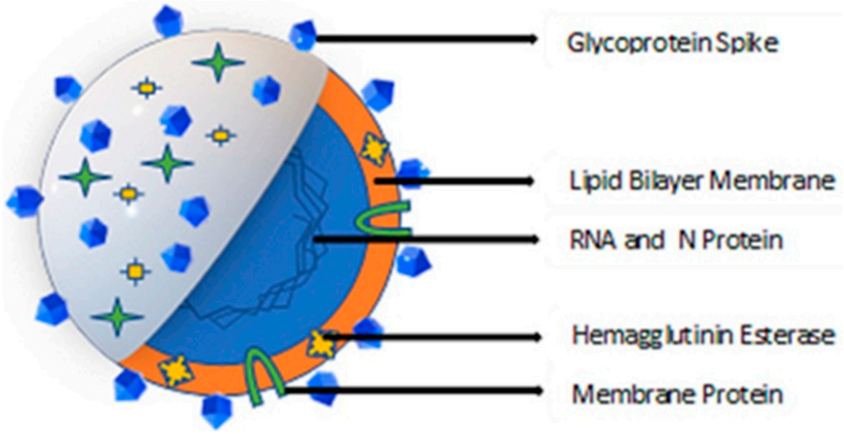


Figure 25. A coronavirus structure [204].

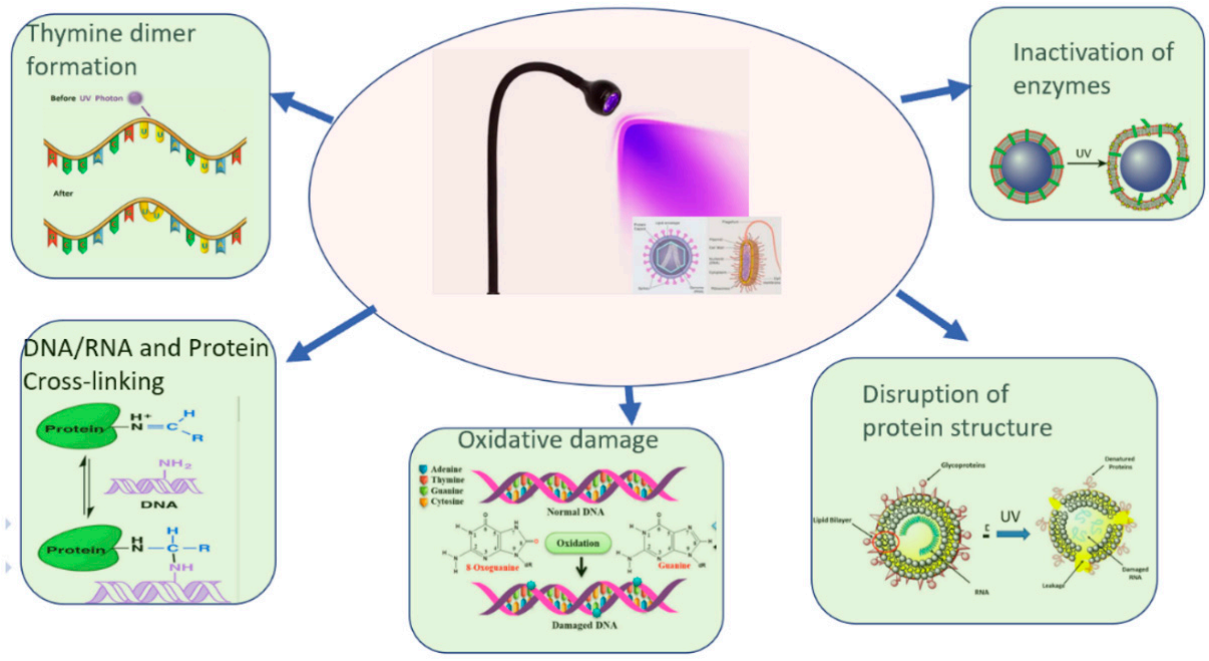


Figure 26. Different mechanisms of microbial deactivation by UV.

5.2.1. Coronavirus Types

Coronaviruses are named because of the crown-like spikes (6–10 nm) on their surface. Some common coronaviruses in humans are (i) 229E (alpha coronavirus); (ii) NL63 (alpha coronavirus); (iii) OC43 (beta coronavirus); and (iv) HKU1 (beta coronavirus). Other types of coronaviruses infecting humans include MERS-CoV, SARS-CoV, and SARS-CoV-2 (COVID-19). As noted earlier, various studies have shown that UV-C LEDs are effective in deactivating coronaviruses. Table 3 displays some of the coronaviruses that can be deactivated at specific wavelengths using different doses of UV radiation.

5.2.2. Microorganism Response to UV Radiation

As noted earlier in several literature reports, UV radiation is highly effective in deactivating microbes. However, diverse microorganisms have revealed different responses to UV light and processing conditions. Generally, the sensitivity of microorganisms to UV light is measured in terms of the inactivation rate constant, k. It can be determined from the relation between the log inactivation (log reduction) and the UV dose [205].

$$\text{Log inactivation} = k \times \text{UV dose} \quad (1)$$

where the value of k is different for the different microorganisms. A higher k-value means that the microorganism is more sensitive to that particular UV radiation and a relatively small dose of UV radiation would deactivate the microbe. For example, the k-value inactivation for bacteriophage φX174 using 255 nm and 280 nm UV-LEDs was found to be 0.578 and 0.360 cm^2/mJ [193], respectively. This means that 255 nm UV radiation will be more effective than 280 nm for bacteriophage φX174 deactivation. The basic statistical equation that can be used to find the log inactivation rate is

$$\text{Log}_{10}\, I = \text{Log}_{10}\, (No/N) \quad (2)$$

where Log_{10} I, is the infectivity/reduction in the $\log_{10}$ scale; N_o and N are the virus sample infectivity rates before and after UV exposure.

To evaluate the effectiveness of UV LED disinfection, the UV dose, and log inactivation data were measured. The log inactivation for disinfection is a mathematical expression used to express the relative number of pathogens killed/eliminated during the disinfection process. For example, 1-log inactivation corresponds to the inactivation of 90% of target pathogens with pathogens counts reduced by a factor of 10 and the inactivation of 99%, 99.9%, 99.99% of pathogens corresponds to 2-, 3-, and 4-log inactivation, respectively.

Table 3. UV dose and wavelength required for the deactivation of various types of coronaviruses.

Viruses	Wavelength (nm)	Sample Condition	UV Dose for log Reduction (mJ/cm^2)	References
HCoV-229E (alpha coronavirus	222	Aerosol	0.56	[206]
OC43 (beta coronavirus)	222	Aerosol	0.39	[206]
MERS-CoV	254	Droplets	No dose information but successfully deactivated	[207]
HCoV-229E	254	Liquid serum cell culture	No dose information but successfully deactivated	[207]
HCoV-OC43	254	Liquid serum cell culture	No dose information but successfully deactivated	[208]
SARS-CoV Hanoi	254	Liquid serum cell culture	22.67	[209]
HCoV-OC43	267	Vero E6 cells	6.8 (for 4-log reduction)	[210]
HCoV-OC43	279	Vero E6 cells	8.7 (for 4-log reduction)	[210]
SARS-CoV	254	Salt solution	No dose information but successfully deactivated	[211]

6. The Future in Designing a UV LED Disinfection System

6.1. Building a Deactivation System for Wealthy and Underprivileged Populations with PV Power

As described earlier, UV LEDs have been proven to be effective for microbial disinfection but developing an efficient, cost-effective system is quite a challenge. The sprouting nature of human-affecting microbes poses global health risks, necessitating urgent solutions. The recent COVID-19 pandemic, emerging variants, and rising cases of other viruses such as Monkeypox highlight the demand for UV LED-based disinfection systems. These offer a superior alternative to chemical methods. In order to address environmental concerns and global accessibility, we have focused on the design of a solar-powered UV LED disinfection system for diverse settings. This renewable energy source can be harnessed worldwide, even in areas lacking grid electricity. The goal is to develop a self-contained, portable UV LED system accessible to all, including regions with limited electricity access. The envisioned system incorporates a solar-powered charging mechanism and a rechargeable battery for nighttime operation. Figure 27 illustrates the design of a portable rechargeable UV LED unit for disinfection. Its optimization will be necessary for all aspects e.g., cost, efficiency, and portability. In Figure 28, the rudimentary design of a UV LED-based disinfectant system is outlined. This can be installed in larger/open areas such as hospitals, schools, airports, and so on. The proposed system would store power with its large battery capacity and would remain effective for a long time.

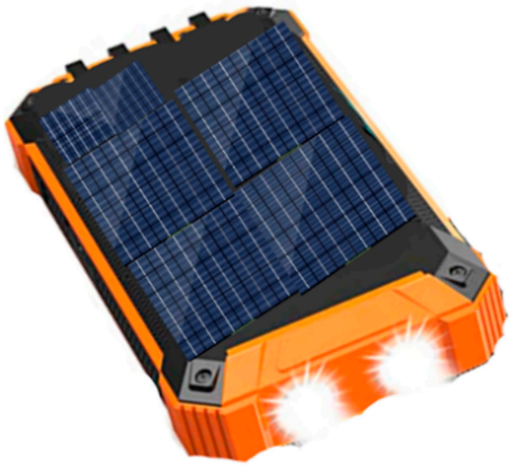


Figure 27. Design of portable and rechargeable solar-powered UV LED disinfectant light.

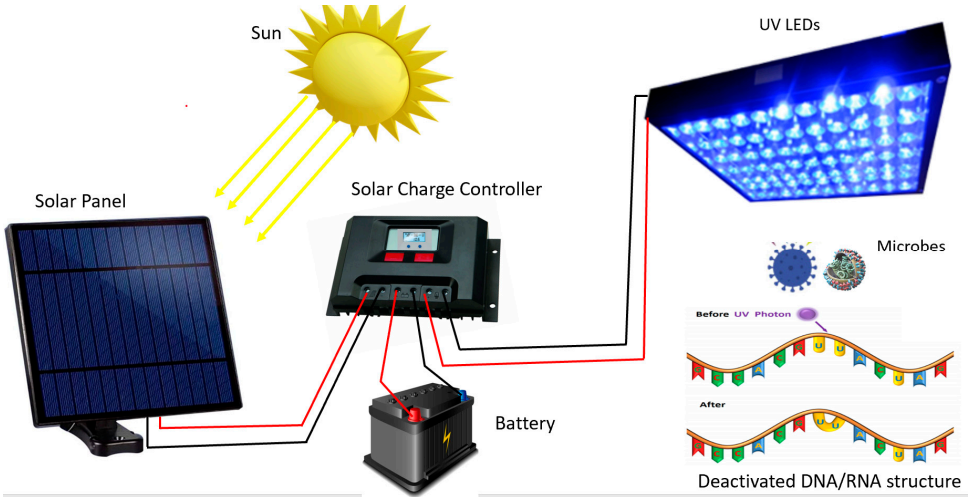


Figure 28. Outline of a solar-powered UV LED system for large area applications.

6.2. Manufacturing of Cost-Effective Portable High-Precision Virus Deactivation System

Designing cost-effective and highly accurate UV LED disinfectants presents significant challenges. The integration of solar modules (cells/wafers), batteries, and UV LED arrays in the basic module, termed "Solar UV-LEDs", is the key area for potential cost reduction. In order to compete with conventional energy sources, advancements in solar power technology must prioritize lowering the cost per kilowatt. This involves minimizing electrical conversion losses, improving cell efficiency, and enhancing manufacturing processes for wafers, cells, and modules. Increasing the production volume and reducing metallization, substrate, and epitaxial growth costs are crucial areas for improvement. An optimal battery design is also essential for efficient energy storage. Recent advances in battery technology offer various lithium-based options, but durability under diverse conditions remains a priority. Research into battery materials and combinations is crucial for longevity and performance. Additionally, cost-effective UV LED disinfection devices can be achieved through the strategic use of LED chips/strips considering material choice and fabrication techniques. The number of UV LED lights used should align with deactivation needs to control costs. Precise design based on factors such as the UV dose, exposure time, and wavelength requirements would further enhance its accuracy and effectiveness.

7. Discussion and Conclusions

We carried out a detailed investigative review of the historical development of UV and RGB LEDs, leaving IR out of the scope of this manuscript. The application of LEDs in the lighting and decoration industry, the agricultural sector, and display technology, with their current trends and future roadmaps, were reviewed and discussed. From our review, we saw that the efficiency of LEDs is continuously increasing. Different design techniques, appropriate material compositions, different deposition techniques, etc., are used to improve the efficiency of LEDs. An overview of applications of LEDs that we discussed above were summarized in Figure 29.

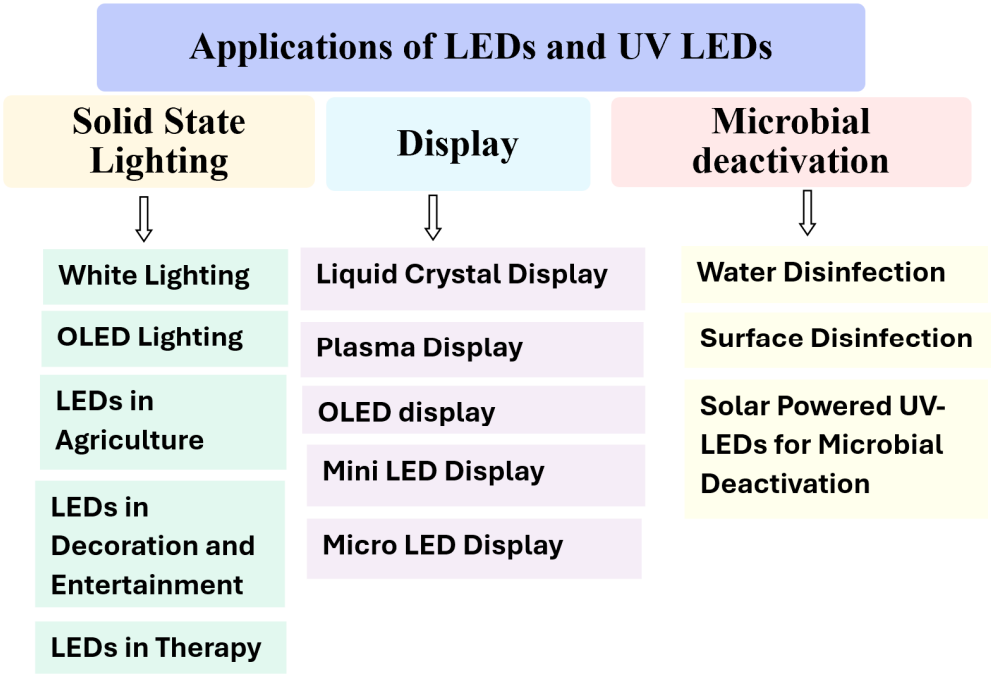


Figure 29. Summary of applications of LEDs and UV LEDs.

From our review, we conclude that the demand for LEDs is on the ascent, and their applications in lighting, agriculture, and display technology are still in the growing stage. Micro-LED display technology could possibly revolutionize the display market in the future. Further research into and development of LEDs in agriculture would significantly

improve crop production quality and frequency. The lighting industry is still advancing, with new developments in the decoration and entertainment sectors as well.

A thorough review and analysis of UV LED applications in microbial disinfection was conducted while leaving other industrial applications out of the discussion. Based on the literature review and analyses of UV LEDs and the response of microorganisms to UV light, we conclude that UV radiation is highly effective in deactivating various microorganisms.

However, the results of the reported experiments do not yet seem consistent. The diverse parameters e.g., UV dose, wavelength, and the exposure time required for the wide range of microbial deactivation scenarios, have not been well established. To date, most of the research regarding the inactivation of microorganisms has been carried out with conventional sources of UV such as mercury vapor lamps. The application of high-efficiency UV LEDs will be precise and effective. Determining the most effective wavelength, UV dose and exposure time for deactivation has huge application potential in disinfection methodology. UV LEDs disinfection can be applied to water purification and as a surface disinfectant as well as in various medical applications. If a multiple-wavelengths UV LED system is developed, it would be a 'death trap' for a large range of microbes. This would revolutionize surface disinfection and water and air purification research and applications.

Furthermore, UV LEDs powered with solar modules and a self-sustained design have also been summarized. This will help in applying it to numerous applications, especially as a surface disinfectant. They will readily find applications in numerous areas such as airports, hospitals, and schools, as well as homes. Likewise, if one could develop a portable module, it would be highly useful in any part of the world with limited or no electricity. We also presented an outline of the design of a UV LED disinfectant system. The most efficient system and optimum design should be built based on the power required to light-up a UV LED, the solar energy absorbed by solar cells, and the storage capacity of the battery used. Another possible application of this device in computing is the development of smart disinfection systems. By integrating UV LED systems with sensors, Internet-of-Things (IoT) devices, and artificial intelligence algorithms, disinfection could become more targeted and efficient. To summarize the discussion, we can confidently say that there is tremendous potential and scope for developing a solar-powered UV LED system that will be effective in destroying microorganisms and UV LED-based disinfectant technology could be revolutionized.

Author Contributions: Idea generation, literature review, draft preparation writing and editing by T.B.; idea generation, reviewing, editing and supervision by A.E. and M.Y.A.R. All authors have read and agreed to the published version of the manuscript.

Funding: No external funding was provided.

Data Availability Statement: Not applicable.

Conflicts of Interest: The authors declare no conflicts of interest.

References

1. Lu, X.; Hua, T.; Wang, Y. Thermal analysis of high-power LED package with heat pipe heat sink Heat pipe. *Microelectron. J.* **2011**, *42*, 1257–1262. [CrossRef]
2. Novikov, M.A. Oleg Vladimirovich Losev: Pioneer of semiconductor electronics (celebrating one hundred years since his birth). *Phys. Solid State* **2004**, *46*, 1–4. [CrossRef]
3. Yurchuk, S.; Rabinovich, O.; Didenko, S. LED and Phototransistor Simulation. In *Optoelectronics-Advanced Device Structures*; Pyshkin, S., Ballato, J., Eds.; IntechOpen: Rijeka, Croatia, 2017; pp. 50–51.
4. Phillips, J.; Coltrin, M.; Crawford, M.; Fischer, A.; Krames, M.; Mueller-Mach, R.; Mueller, G.; Ohno, Y.; Rohwer, L.; Simmons, J.; et al. Research challenges to ultra-efficient inorganic solid-state lighting. *Laser Photon. Rev.* **2007**, *1*, 307–333. [CrossRef]
5. Weisbuch, C. On the search for efficient solid state light emitters: Past, present, future. *ECS J. Solid State Sci. Technol.* **2020**, *9*, 016022. [CrossRef]
6. Rahman, F. Solid-state lighting with wide bandgap semiconductors. *MRS Energy Sustain.* **2014**, *1*, E6. [CrossRef]
7. Maraj, M.; Min, L.; Sun, W. Reliability analysis of AlGaN-based deep UV-LEDs. *Nanomaterials* **2022**, *12*, 3731. [CrossRef] [PubMed]
8. Chayed, N.F.; Badar, N.; Rusdi, R.; Kamarudin, N.; Kamarulzaman, N. Optical bandgap energies of magnesium oxide (MgO) thin film and spherical nanostructures. *AIP Conf. Proc.* **2011**, *1400*, 328–332.

9. Li, S.; Chen, H.; Wang, W.; Yao, D.; Xia, Y.; Zeng, Y. Effects of Y_2O_3 /MgO ratio on mechanical properties and thermal conductivity of silicon nitride ceramics. *Int. J. Appl. Ceram. Technol.* **2022**, *19*, 2873–2882.
10. Malinauskas, T.; Jarašiūnas, K.; Aleksiejunas, R.; Gogova, D.; Monemar, B.; Beaumont, B.; Gibart, P. Contribution of dislocations to carrier recombination and transport in highly excited ELO and HVPE GaN layers. *Phys. Status Solidi (B)* **2006**, *243*, 1426–1430. [CrossRef]
11. Vennéguès, P.; Beaumont, B.; Bousquet, V.; Vaille, M.; Gibart, P. Reduction mechanisms for defect densities in GaN using one-or two-step epitaxial lateral overgrowth methods. *J. Appl. Phys.* **2000**, *87*, 4175–4181. [CrossRef]
12. Malinauskas, T.; Aleksiejūnas, R.; Jarašiūnas, K.; Beaumont, B.; Gibart, P.; Kakanakova-Georgieva, A.; Janzén, E.; Gogova, D.; Monemar, B.; Heuken, M. All-optical characterization of carrier lifetimes and diffusion lengths in MOCVD-, ELO-, and HVPE-grown GaN. *J. Cryst. Growth* **2007**, *300*, 223–227. [CrossRef]
13. Schmidt, M.; Kim, K.; Sato, H.; Fellows, N.; Masui, H.; Nakamura, S.; DenBaars, S.; Speck, J. High power and high external efficiency m-plane InGaN light emitting diodes. *Jpn. J. Appl. Phys.* **2007**, *46*, L126. [CrossRef]
14. Riechert, H.; Averbeck, R.; Graber, A.; Schienle, M.; Strau, U. MBE growth of (In) GaN for LED applications. *MRS Online Proc. Libr.* **1996**, *449*, 149. [CrossRef]
15. Islam, S.M.; Lee, K.; Verma, J.; Protasenko, V.; Rouvimov, S.; Bharadwaj, S.; Jena, D. MBE-grown 232–270 nm deep-UV LEDs using monolayer thin binary GaN/AlN quantum heterostructures. *Appl. Phys. Lett.* **2017**, *110*, 041108. [CrossRef]
16. Chen, S.W.; Li, H.; Lu, T.C. Improved performance of GaN based light emitting diodes with ex-situ sputtered AlN nucleation layers. *AIP Adv.* **2016**, *6*, 045311. [CrossRef]
17. Borchardt, J.K. Developments in organic displays. *Mater. Today* **2004**, *7*, 42–46. [CrossRef]
18. Lin, D.W.; Lin, C.C.; Chiu, C.H.; Lee, C.Y.; Yang, Y.Y.; Li, Z.Y.; Lai, W.C.; Lu, T.C.; Kuo, H.C.; Wang, S.C. GaN-based LEDs grown on HVPE growth high crystalline quality thick GaN template. *J. Electrochem. Soc.* **2011**, *158*, H1103. [CrossRef]
19. Siekacz, M.; Szańkowska, M.L.; Feduniewicz-Zmuda, A.; Smalc-Koziorowska, J.; Cywiński, G.; Grzanka, S.; Wasilewski, Z.R.; Grzegory, I.; Łucznik, B.; Porowski, S.; et al. InGaN light emitting diodes for 415 nm–520 nm spectral range by plasma assisted MBE. *Phys. Status Solidi C* **2009**, *6*, S917–S920. [CrossRef]
20. Marko, I.; Jin, S.; Hild, K.; Batool, Z.; Bushell, Z.; Ludewig, P.; Stolz, W.; Volz, K.; Butkutė, R.; Pačebutas, V.; et al. Properties of hybrid MOVPE/MBE grown GaAsBi/GaAs based near-infrared emitting quantum well lasers. *Semicond. Sci. Technol.* **2015**, *30*, 094008. [CrossRef]
21. Chunlan, M.; Wenqing, F.; Hechu, L. Growth and characterization of InGaN blue LED structure on Si (111) by MOCVD. *J. Cryst. Growth* **2005**, *285*, 312–317.
22. Nguyen, X.; Nguyen, T.; Chau, V.; Dang, C. The fabrication of GaN-based light emitting diodes (LEDs). *Adv. Nat. Sci. Nanosci. Nanotechnol.* **2010**, *1*, 025015. [CrossRef]
23. Xu, T.; Nikiforov, A.Y.; France, R.; Thomidis, C.; Williams, A.; Moustakas, T.D. 2007. Blue-green-red LEDs based on InGaN quantum dots grown by plasma-assisted molecular beam epitaxy. *Phys. Status Solidi (A)* **2007**, *204*, 2098–2102. [CrossRef]
24. Matsunami, H.I.; Ikeda, M.I.; Suzuki, A.K.; Tanaka, T.E. SiC blue LED's by liquid-phase epitaxy. *IEEE Trans. Electron. Devices* **1977**, *24*, 958–961. [CrossRef]
25. Yu, H.; Wang, S.; Li, N.; Fenwick, W.; Melton, A.; Klein, B.; Ferguson, I. MOVPE growth of AlGaN/GaN superlattices on ZnO substrates for green emitter applications. *J. Cryst. Growth* **2008**, *310*, 4904–4907. [CrossRef]
26. Craford, M.G.; Groves, W.O. Vapor phase epitaxial materials for LED applications. *Proc. IEEE* **1973**, *61*, 862–880. [CrossRef]
27. Kong, Y.C.; Yu, D.P.; Zhang, B.; Fang, W.; Feng, S.Q. Ultraviolet-emitting ZnO nanowires synthesized by a physical vapor deposition approach. *Appl. Phys. Lett.* **2001**, *78*, 407–409. [CrossRef]
28. Nakamura, S. III–V nitride based light-emitting devices. *Solid State Commun.* **1997**, *102*, 237–248. [CrossRef]
29. Rahman, F. Zinc oxide light-emitting diodes: A review. *Opt. Eng.* **2019**, *58*, 010901. [CrossRef]
30. Ishibashi, A. II–VI blue-green light emitters. *J. Cryst. Growth* **1996**, *159*, 555–565. [CrossRef]
31. Lu, S.C.; Wu, M.C.; Lee, C.Y.; Yang, Y.C. Liquid-phase epitaxial growth of InGaP for red electroluminescent devices. *Solid State Electron.* **1991**, *34*, 843–851. [CrossRef]
32. Mukai, T.; Morita, D.; Nakamura, S. High-power UV InGaN/AlGaN double-heterostructure LEDs. *J. Cryst. Growth* **1998**, *189–190*, 778–781. [CrossRef]
33. Hirayama, H.; Yatabe, T.; Noguchi, N.; Kamata, N. Development of 230–270 nm AlGaN-based deep-UV LEDs. *Electron. Commun. Jpn.* **2010**, *93*, 24–33. [CrossRef]
34. Sun, X.W.; Ling, B.; Zhao, J.L.; Tan, S.T.; Yang, Y.; Shen, Y.Q.; Dong, Z.L.; Li, X.C. Ultraviolet emission from a ZnO rod homojunction light-emitting diode. *Appl. Phys. Lett.* **2009**, *95*, 133124. [CrossRef]
35. Evseenkov, A.S.; Tarasov, S.A.; Lamkin, I.A.; Solomonov, A.V.; Kurin, S.Y. The efficiency of UV LEDs based on GaN/AlGaN heterostructures. In Proceedings of the 2015 IEEE NW Russia Young Researchers in Electrical and Electronic Engineering Conference (EIConRusNW), St. Petersburg, Russia, 2–4 February 2015; pp. 27–29.
36. Eason, D.; Ren, J.; Yu, Z.; Hughes, C.; Cook, J.W., Jr.; Schetzina, J.F.; El-Masry, N.A.; Cantwell, G.; Harsh, W.C. Blue and green light-emitting diode structures grown by molecular beam epitaxy on ZnSe substrates. *J. Cryst. Growth* **1995**, *150*, 718–724. [CrossRef]
37. Su, Y.K.; Wu, M.C.; Chang, C.Y.; Cheng, K.Y. The fabrication of single heterojunction AlGaAs/InGaP electroluminescent diodes. *J. Appl. Phys.* **1987**, *62*, 2541–2544. [CrossRef]

38. Baldo, M.A.; O'Brien, D.; You, Y.; Shoustikov, A.; Sibley, S.P.; Thompson, M.E.; Forrest, S.R. Highly efficient phosphorescent emission from organic electroluminescent devices. *Nature* **1998**, *395*, 151–154. [CrossRef]
39. Pal, B.; Ghosh, Y.; Brovelli, S.; Laocharoensuk, R.; Klimov, V.; Hollingsworth, J.; Htoon, H. 'Giant' CdSe/CdS core/shell Nanocrystal Quantum Dots as Efficient Electroluminescent Materials: Strong Influence of Shell Thickness on Light-Emitting Diode Performance. *Nano Lett.* **2011**, *12*, 331–336. [CrossRef] [PubMed]
40. Kim, Y.; Cho, H.; Heo, J.; Kim, T.; Myoung, N.; Lee, C.; Im, L.; Lee, W. Multicolored organic/inorganic hybrid perovskite light-emitting diodes. *Adv. Mater.* **2014**, *27*, 1248–1254. [CrossRef]
41. Jung, B.; Lee, W.; Kim, J.; Choi, M.; Shin, H.; Joo, M.; Jung, S.; Choi, Y.; Kim, M. Enhancement in external quantum efficiency of AlGaNP red μ-led using chemical solution treatment process. *Sci. Rep.* **2021**, *11*, 4535. [CrossRef]
42. Sutherland, B.R. Perovskite photonic sources. *Nat. Photonics* **2016**, *10*, 295–302. [CrossRef]
43. Kwak, J.; Bae, W.; Lee, D.; Park, I.; Lim, J.; Park, M.; Cho, H.; Woo, H.; Yoon, D.; Char, K.; et al. Bright and efficient full-color colloidal quantum dot light-emitting diodes using an inverted device structure. *Nano Lett.* **2012**, *12*, 2362–2366. [CrossRef] [PubMed]
44. Leyden, M.; Meng, L.; Jiang, Y.; Ono, L.; Qiu, L.; Juárez-Pérez, E.; Qin, C.; Adachi, C.; Qi, Y. Methylammonium lead bromide perovskite light-emitting diodes by chemical vapor deposition. *J. Phys. Chem. Lett.* **2017**, *8*, 3193–3198. [CrossRef] [PubMed]
45. Jagadhane, K.; Butcher, R.; Dongale, T.; Nirmal, K.; Kolekar, G.; Tamboli, M.; Kim, T.; Salunke-Gawali, S.; Anbhule, P. Multifunctional fluorescent tetraphenylethene-based reversible mechanochromism for highly selective detection of MnO_4^- in aqueous media and green organic light emitting diode applications. *Cryst. Growth Des.* **2023**, *23*, 4164–4179. [CrossRef]
46. Uthirakumar, P.; Hong, C.; Suh, E.K.; Lee, Y. Novel fluorescent polymer/zinc oxide hybrid particles: synthesis and application as a luminescence converter for white light-emitting diodes. *Chem. Mater.* **2006**, *18*, 4990–4992. [CrossRef]
47. Zheng, H.; Zheng, Y.; Liu, N.; Ai, N.; Wang, Q.; Wu, S.; Zhou, J.; Hu, D.; Yu, S.; Han, S.; et al. All-solution processed polymer light-emitting diode displays. *Nat. Commun.* **2013**, *4*, 1971. [CrossRef] [PubMed]
48. Jeon, S.; Jang, S.; Son, H.; Lee, J. External quantum efficiency above 20% in deep blue phosphorescent organic light-emitting diodes. *Adv. Mater.* **2011**, *23*, 1436–1441. [CrossRef] [PubMed]
49. Huang, S.; Yu, Y.; Shang, M.; Sun, Y.; Dang, P.; Lin, J. Super broadband near-infrared solid solution phosphors with adjustable peak wavelengths from 1165 to 875 nm for NIR spectroscopy applications. *Adv. Opt. Mater.* **2023**, *11*, 2202291. [CrossRef]
50. Luo, X.; Xiong, W.; Cheng, T.; Liu, S. Temperature estimation of high-power light emitting diode streetlamp by a multi-chip analytical solution. *IET Optoelectron.* **2009**, *3*, 225–232. [CrossRef]
51. Arık, M.; Becker, C.; Weaver, S.; Petroski, J. Thermal management of LEDs: Package to system. *SPIE Proc.* **2004**, *5187*, 64–75.
52. Wang, R.; Wang, J. Analyzing the structural designs and thermal performance of nonmetal lighting devices of led bulbs. *Int. J. Heat Mass Transfer.* **2016**, *99*, 750–761. [CrossRef]
53. Chuluunbaatar, Z.; Kim, N.Y. Thermal analysis and optimization of 6.4 w Si-based multichip led packaged module. *J. Korean Inst. Commun. Sci.* **2014**, *39*, 234–238. [CrossRef]
54. Hong, D.; Lee, S. A study on high power led lamp structures. *Korean J. Opt. Photon.* **2010**, *21*, 118–122. [CrossRef]
55. Kang, S.; Moon, D.; Jang, J.; Kim, J.; Suh, J.; Yoon, E.; Han, H.; Choi, I. Flaw-containing alumina hollow nanostructures have ultrahigh fracture strength to be incorporated into high-efficiency GaN light-emitting diodes. *Nano Lett.* **2018**, *18*, 1323–1330. [CrossRef] [PubMed]
56. Özgür, U.; Alivov, Y.I.; Liu, C.; Teke, A.; Reshchikov, M.A.; Doğan, S.; Avrutin, V.C.S.J.; Cho, S.J.; Morkoç, A. A comprehensive review of ZnO materials and devices. *J. Appl. Phys.* **2005**, *98*, 041301. [CrossRef]
57. Priller, H.; Brückner, J.; Gruber, T.; Klingshirn, C.; Kalt, H.; Waag, A.; Ko, H.; Yao, T. Comparison of linear and nonlinear optical spectra of various ZnO epitaxial layers and of bulk material obtained by different experimental techniques. *Phys. Status Solidi (B)* **2004**, *241*, 587–590. [CrossRef]
58. Bavencove, A.; Salomon, D.; Lafossas, M.; Martin, B.; Dussaigne, A.; Lévy, F.; Andre, B.; Ferret, P.; Durand, C.; Eymery, J.; et al. Light emitting diodes based on GaN core/shell wires grown by MOVPE on n-type Si substrate. *Electron. Lett.* **2011**, *47*, 765–767. [CrossRef]
59. Gong, X.; Kan, H.; Makino, T.; Watanabe, K.; Iida, T.; Suzuki, H.; Aoyama, M.; Yamaguchi, T. Light emitting diodes fabricated from liquid phase epitaxial $InAs/InAs_xP_{1-x-y}Sb_y$/ $InAs/InAs_{x'}P_{1-x'-y'}Sb_{y'}$' and $InAs/InAs_{1-x}Sb_x$ multi-layers. *Cryst. Res. Technol.* **2000**, *35*, 549–555. [CrossRef]
60. Noorprajuda, M.; Ohtsuka, M.; Adachi, M.; Fukuyama, H. AlN formation by an Al/GaN substitution reaction. *Sci. Rep.* **2020**, *10*, 13058. [CrossRef] [PubMed]
61. Akasaki, I.; Amano, H.; Murakami, H.; Sassa, M.; Kato, H.; Manabe, K. Growth of GaN and AlGaN for UV/blue p-n junction diodes. *J. Cryst. Growth* **1993**, *128*, 379–383. [CrossRef]
62. Edmond, J.; Abare, A.; Bergman, M.; Bharathan, J.; Bunker, K.; Emerson, D.; Haberern, K.; Ibbetson, J.; Leung, M.; Russel, P.; et al. High efficiency GaN-based LEDs and lasers on SiC. *J. Cryst. Growth* **2004**, *272*, 242–250. [CrossRef]
63. Muramoto, Y.; Kimura, M.; Nouda, S. Development and future of ultraviolet light-emitting diodes: UV-LED will replace the UV lamp. *Semicond. Sci. Technol.* **2014**, *29*, 084004. [CrossRef]
64. Oh, J.; Moon, Y.; Kang, D.; Park, C.; Han, J.; Jung, M.; Sung, Y.; Jeong, H.; Song, J.; Seong, T. High efficiency ultraviolet GaN-based vertical light emitting diodes on 6-inch sapphire substrate using ex-situ sputtered AlN nucleation layer. *Opt. Express* **2018**, *26*, 5111–5117. [CrossRef] [PubMed]

65. Li, Y.; Xing, Z.; Zheng, Y.; Tang, X.; Xie, W.; Chen, X.; Wang, W.; Li, G. High-efficiency near-UV light-emitting diodes on Si substrates with InGaN/GaN/AlGaN/GaN multiple quantum wells. *J. Mater. Chem. C* **2020**, *8*, 883–888. [CrossRef]
66. Shur, M.S.; Gaska, R. Deep-Ultraviolet Light-Emitting Diodes. *IEEE Trans. Electron. Devices* **2010**, *57*, 12–25. [CrossRef]
67. Hirayama, H.; Fujikawa, S.; Noguchi, N.; Norimatsu, J.; Takano, T.; Tsubaki, K.; Kamata, N. 222-282 nm AlGaN and InAlGaN-based deep-UV LEDs fabricated on high-quality AlN on sapphire. *Phys. Status Solidi A* **2009**, *206*, 1176–1182. [CrossRef]
68. Fujioka, A.; Misaki, T.; Murayama, T.; Narukawa, Y.; Mukai, T. Improvement in Output Power of 280-nm Deep Ultraviolet Light-Emitting Diode by Using AlGaN Multi Quantum Wells. *Appl. Phys. Express* **2010**, *3*, 041001. [CrossRef]
69. Shatalov, M.; Sun, W.; Lunev, A.; Hu, X.; Dobrinsky, A.; Bilenko, Y.; Yang, J.; Shur, M.; Gaska, R.; Moe, C.; et al. AlGaN Deep-Ultraviolet Light-Emitting Diodes with External Quantum Efficiency above 10%. *Appl. Phys. Express* **2012**, *5*, 082101. [CrossRef]
70. Takano, T.; Mino, T.; Sakai, J.; Noguchi, N.; Tsubaki, K.; Hirayama, H. Deep-ultraviolet light-emitting diodes with external quantum efficiency higher than 20% at 275 nm achieved by improving light-extraction efficiency. *Appl. Phys. Express* **2017**, *10*, 031002. [CrossRef]
71. Maeda, N.; Jo, M.; Hasegawa, H. Improving the Efficiency of AlGaN Deep-UV LEDs by Using Highly Reflective Ni/Al p-Type Electrodes. *Phys. Status Solidi A* **2018**, *215*, 1700435. [CrossRef]
72. Pandey, A.; Shin, W.; Gim, J.; Hovden, R.; Mi, Z. High-efficiency AlGaN/GaN/AlGaN tunnel junction ultraviolet light-emitting diodes. *Photon. Res.* **2020**, *8*, 331–337. [CrossRef]
73. Zheng, Z.; Chen, Q.; Dai, J.; Wang, A.; Liang, R.; Zhang, Y.; Shan, M.; Wu, F.; Zhang, W.; Chen, C.; et al. Enhanced light extraction efficiency via double nano-pattern arrays for high-efficiency deep UV LEDs. *Opt. Laser Technol.* **2021**, *143*, 107360. [CrossRef]
74. Chen, K.; Dai, Q.; Lee, W.; Kim, J.; Schubert, E.; Grandusky, J.; Mendrick, M.; Li, X.; Smart, J. Effect of dislocations on electrical and optical properties of n-type $Al_{0.34}Ga_{0.66}N$. *Appl. Phys. Lett.* **2008**, *93*, 192108. [CrossRef]
75. Nam, K.B.; Li, J.; Nakarmi, M.L.; Lin, J.Y.; Jiang, H.X. Unique optical properties of AlGaN alloys and related ultraviolet emitters. *Appl. Phys. Lett.* **2004**, *84*, 5264–5266. [CrossRef]
76. Kuo, Y.-K.; Chang, J.-Y.; Chen, F.-M.; Shih, Y.-H.; Chang, H.-W. Numerical Investigation on the Carrier Transport Characteristics of AlGaN Deep-UV Light-Emitting Diodes. *IEEE J. Quantum Electron.* **2016**, *52*, 1–5. [CrossRef]
77. Chitnis, A.; Sun, J.; Mandavilli, V.; Pachipulusu, R.; Wu, S.; Gaevski, M.; Adivarahan, V.; Zhang, J.; Khan, M.; Sarua, A. Kuball, M. Self-heating effects at high pump currents in deep ultraviolet light-emitting diodes at 324 nm. *Appl. Phys. Lett.* **2002**, *81*, 3491–3493. [CrossRef]
78. Mondal, R.K.; Adhikari, S.; Chatterjee, V.; Pal, S. Recent advances and challenges in AlGaN-based ultra-violet light emitting diode technologies. *Mater. Res. Bull.* **2021**, *140*, 111258. [CrossRef]
79. Chadi, D.J. Doping in ZnSe, ZnTe, MgSe, MgTe wide-bandgap semiconductors. *Phys. Rev. Lett.* **1994**, *72*, 534. [CrossRef]
80. Gogova, D.; Kasic, A.; Larsson, H.; Pécz, B.; Yakimova, R.; Magnusson, B.; Monemar, B.; Tuomisto, F.; Saarinen, K.; Miskys, C.; et al. Optical and structural characteristics of virtually unstrained bulk-like GaN. *J. Appl. Phys.* **2004**, *43*, 1264. [CrossRef]
81. Ned, A. Why Blue LED Earned a Nobel Prize if Reds and Greens Already Existed for Decades? In Predict: 10 March 2021. Available online: https://medium.com/predict/why-blue-led-earned-nobel-prize-if-reds-and-greens-already-existed-for-decades-d03e31a6fd8f (accessed on 15 January 2024).
82. Nakamura, S.; Senoh, M.; Mukai, T. P-GaN/N-InGaN/N-GaN Double-Heterostructure Blue-Light-Emitting Diodes. *Jpn. J. Appl. Phys.* **1993**, *32*, L8–L11. [CrossRef]
83. Craford, M.G. From Holonyak to Today. *Proc. IEEE* **2013**, *101*, 2170–2175. [CrossRef]
84. Brahmbhatt, G. Blue LEDs Will Have a Significant Positive Impact on Lighting Costs & the Environment. Available online: https://www.bisinfotech.com/blue-leds-will-have-a-significant-positive-impact-on-lighting-costs-the-environment/ (accessed on 20 January 2024).
85. Krames, M.; Shchekin, O.; Mueller-Mach, R.; Mueller, G.; Zhou, L.; Harbers, G.; Craford, M. Status and Future of High-Power Light-Emitting Diodes for Solid-State Lighting. *J. Disp. Technol.* **2007**, *3*, 160–175. [CrossRef]
86. Nakamura, S.; Mukai, T.; Senoh, M.; Iwasa, N. Thermal Annealing Effects on P-Type Mg-Doped GaN Films. *Jpn. J. Appl. Phys.* **1992**, *31*, L139–L142. [CrossRef]
87. Nakamura, S.; Iwasa, N.; Masayuki Senoh, M.S.; Takashi Mukai, T.M. Hole Compensation Mechanism of P-Type GaN Films. *Jpn. J. Appl. Phys.* **1992**, *31*, 1258. [CrossRef]
88. Amano, H.; Kito, M.; Hiramatsu, K.; Akasaki, I. P-Type Conduction in Mg-Doped GaN Treated with Low-Energy Electron Beam Irradiation (LEEBI). *Jpn. J. Appl. Phys.* **1989**, *28*, L2112–L2114. [CrossRef]
89. Nakamura, S.; Mukai, T. High-Quality InGaN Films Grown on GaN Films. *Jpn. J. Appl. Phys.* **1992**, *31*, L1457–L1459. [CrossRef]
90. Nakamura, S. GaN Growth Using GaN Buffer Layer. *Jpn. J. Appl. Phys.* **1991**, *30*, L1705–L1707. [CrossRef]
91. Amano, H.; Sawaki, N.; Akasaki, I.; Toyoda, Y. Metalorganic vapor phase epitaxial growth of a high quality GaN film using an AlN buffer layer. *Appl. Phys. Lett.* **1986**, *48*, 353–355. [CrossRef]
92. Kimura, S.; Yoshida, H.; Uesugi, K.; Ito, T.; Okada, A.; Nunoue, S. Performance enhancement of blue light-emitting diodes with InGaN/GaN multi-quantum wells grown on Si substrates by inserting thin AlGaN interlayers. *J. Appl. Phys.* **2016**, *120*, 113104. [CrossRef]
93. Hou, S.; Gangishetty, M.K.; Quan, Q.; Congreve, D.N. Efficient blue and white perovskite light-emitting diodes via manganese doping. *Joule* **2018**, *2*, 2421–2433. [CrossRef]

94. Vashishtha, P.; Ng, M.; Shivarudraiah, S.B.; Halpert, J.E. High efficiency blue and green light-emitting diodes using Ruddlesden–Popper inorganic mixed halide perovskites with butylammonium interlayers. *Chem. Mater.* **2018**, *31*, 83–89. [CrossRef]
95. The History of LED Lighting—Energysavinglighting.org. 19 November 2019. Available online: https://www.energysavinglighting.org/the-history-of-led-lighting/ (accessed on 16 January 2024).
96. Bush, S. 50 Year History of the LED. Electronics Weekly. 22 September 2010. Available online: https://www.electronicsweekly.com/news/products/led/50-year-history-of-the-led-2-2010-09/#:~:text=With%20his%20PhD%20from%20Illinois (accessed on 16 January 2024).
97. Akasaki, I. Fascinating journeys into blue light (Nobel Lecture). *Ann. Phys.* **2015**, *527*, 311–326. [CrossRef]
98. Eason, D.B.; Yu, Z.; Hughes, W.C.; Roland, W.H.; Boney, C.; Cook, J.W., Jr.; Schetzina, J.F.; Cantwell, G.; Harsch, W.C. High-brightness blue and green light-emitting diodes. *Appl. Phys. Lett.* **1995**, *66*, 115–117. [CrossRef]
99. Nakamura, S. Present performance of InGaN-based blue/green/yellow LEDs. *Proc. SPIE* **1997**, *3002*, 26–35.
100. Peter, M.; Laubsch, A.; Bergbauer, W.; Meyer, T.; Sabathil, M.; Baur, J.; Hahn, B. New developments in green LEDs. *Phys. Status Solidi A* **2009**, *206*, 1125–1129. [CrossRef]
101. 3M Claims Record Efficacy for Green LEDs. Technology. 28 July 2010. Available online: https://www.led-professional.com/technology/light-generation/3m-claims-record-efficacy-for-green-leds (accessed on 17 January 2024).
102. Yan, C.; Bai, S.; Nie, T.; Wang, V. High-power high-efficiency green LEDs. In Proceedings of the 2015 12th China International Forum on Solid State Lighting (SSLCHINA), Shenzhen, China, 2–4 November 2015; pp. 1–3.
103. Alhassan, A.I.; Farrell, R.M.; Saifaddin, B.; Mughal, A.; Wu, F.; DenBaars, S.P.; Nakamura, S.; Speck, J.S. High luminous efficacy green light-emitting diodes with AlGaN cap layer. *Opt. Express* **2016**, *24*, 17868–17873. [CrossRef]
104. Li, P.P.; Zhao, Y.B.; Li, H.J.; Che, J.M.; Zhang, Z.H.; Li, Z.C.; Zhang, Y.Y.; Wang, L.C.; Liang, M.; Yi, X.Y.; et al. Very high external quantum efficiency and wall-plug efficiency 527 nm InGaN green LEDs by MOCVD. *Opt. Express* **2018**, *26*, 33108–33115. [CrossRef]
105. Hu, X.; Xiao, F.; Zhou, Q.; Zheng, Y.; Liu, W. High-luminous efficacy green light-emitting diodes with InGaN/GaN quasi-superlattice interlayer and Al-doped indium tin oxide film. *J. Alloys Compd.* **2019**, *794*, 137–143. [CrossRef]
106. Wright, A.; Nelson, J.M. Consistent structural properties for AlN, GaN, and InN. *Phys. Rev. B* **1995**, *51*, 7866–7869. [CrossRef]
107. Zhuang, Z.; Iida, D.; Ohkawa, K. InGaN-based red light-emitting diodes: From traditional to micro-LEDs. *Jpn. J. Appl. Phys.* **2021**, *61*, SA0809. [CrossRef]
108. Iwasaki, Y.; Motomura, G.; Tsuzuki, T. Pure-colored red, green, and blue quantum dot light-emitting diodes using emitting layers composed of cadmium-free quantum dots and organic electron-transporting materials. *Jpn. J. Appl. Phys* **2022**, *61*, 052004. [CrossRef]
109. Holonyak, N.; Bevacqua, S.F. Coherent (visible) light emission from Ga ($As_{1-x}P_x$) junctions. *Appl. Phys. Lett.* **1962**, *1*, 82–83. [CrossRef]
110. Gershenzon, M.; Logan, R.A.; Nelson, D.F. Electrical and Electroluminescent Properties of Gallium Phosphide Diffused p-n Junctions. *Phys. Rev.* **1966**, *149*, 580–597. [CrossRef]
111. Nair, G.B.; Dhoble, S.J. A perspective perception on the applications of light-emitting diodes. *Luminescence* **2015**, *30*, 1167–1175. [CrossRef] [PubMed]
112. Kish, F.A.; Steranka, F.M.; DeFevere, D.C.; Vanderwater, D.A.; Park, K.G.; Kuo, C.P.; Osentowski, T.D.; Peanasky, M.J.; Yu, J.G.; Fletcher, R.M.; et al. Very high-efficiency semiconductor wafer-bonded transparent-substrate($Al_xGa_{1-x})_{0.5}In_{0.5}P$/GaP light-emitting diodes. *Appl. Phys. Lett.* **1994**, *64*, 2839–2841. [CrossRef]
113. Osram Increases LED Efficiency. Photonics Spectra. 28 July 2010. Available online: https://www.photonics.com/Articles/Osram_Increases_LED_Efficiency_/a43266 (accessed on 17 February 2024).
114. 609 nm Red LED Prototype from OSRAM Opto Semiconductors Achieves Record Efficiency. LED Professional—LED Lighting. Technology, Application Magazine. 17 October 2011. Available online: https://www.led-professional.com/technology/light-generation/609-nm-red-led-prototype-from-osram-opto-semiconductors-achieves-record-efficiency (accessed on 11 February 2024).
115. Pattison, P.M.; Hansen, M.; Tsao, J.Y. LED lighting efficacy: Status and directions. *C R. Phys.* **2018**, *19*, 134–145. [CrossRef]
116. Bergh, A.A.; Dean, P.J. Light-emitting diodes. *Proc. IEEE* **1972**, *60*, 156–223. [CrossRef]
117. Bergh, A.A. Bulk degradation of GaP red LEDs. *IEEE Trans. Electron. Devices* **1971**, *18*, 166–170. [CrossRef]
118. 2022 Solid-State Lighting R&D Opportunities. DOE BTO Solid-State Lighting Program, "2022 DOE SSL R&D Opportunities". February 2022. Available online: https://www.energy.gov/eere/ssl/articles/2022-solid-state-lighting-rd-opportunities (accessed on 17 February 2024).
119. Pasayat, S.S.; Gupta, C.; Wong, M.S.; Ley, R.; Gordon, M.J.; DenBaars, S.P.; Nakamura, S.; Keller, S.; Mishra, U.K. Demonstration of ultra-small (<10 μm) 632 nm red InGaN micro-LEDs with useful on-wafer external quantum efficiency (>0.2%) for mini-displays. *Appl. Phys. Express.* **2020**, *14*, 011004.
120. Dussaigne, A.; Le Maitre, P.; Haas, H.; Pillet, J.C.; Barbier, F.; Grenier, A.; Michit, N.; Jannaud, A.; Templier, R.; Vaufrey, D.; et al. Full InGaN red (625 nm) micro-LED (10 μm) demonstration on a relaxed pseudo-substrate. *Appl. Phys. Express* **2021**, *14*, 092011. [CrossRef]

121. Iida, D.; Kirilenko, P.; Velazquez-Rizo, M.; Zhuang, Z.; Najmi, M.A.; Ohkawa, K. Demonstration of 621-nm-wavelength InGaN-based single-quantum-well LEDs with an external quantum efficiency of 4.3% at 10.1 A/cm^2. *AIP Adv.* **2022**, *12*, 065125. [CrossRef]
122. Tan, Z.; Moghaddam, R.; Lai, M.; Docampo, P.; Higler, R.; Deschler, F.; Price, M.; Sadhanala, A.; Pazos, L.M.; Credgington, D.; et al. Bright light-emitting diodes based on organometal halide perovskite. *Nat. Nanotech.* **2014**, *9*, 687–692. [CrossRef] [PubMed]
123. Wang, N.; Mei, T.; Yang, X.; Li, H.; Zhu, N.; Zhang, M. Local doping modulation for improving quantum efficiency in gan-based light-emitting diodes. *Jpn. J. Appl. Phys.* **2013**, *52*, 112102. [CrossRef]
124. Bae, W.; Park, Y.; Lim, J.; Lee, D.; Padilha, L.; McDaniel, H.; Robel, I.; Lee, C.; Pietryga, J.; Klimov, V. Controlling the influence of auger recombination on the performance of quantum-dot light-emitting diodes. *Nat. Commun.* **2013**, *4*, 2661. [CrossRef] [PubMed]
125. Lu, M.; Zhang, X.; Zhang, Y.; Guo, J.; Shen, X.; Yu, W.; Rogach, A. Simultaneous strontium doping and chlorine surface passivation improve luminescence intensity and stability of cspbi3 nanocrystals enabling efficient light-emitting devices. *Adv. Mater.* **2018**, *30*, 1804691. [CrossRef] [PubMed]
126. Bierhuizen, S.; Krames, M.; Harbers, G.; Weijers, G. Performance and trends of high power light emitting diodes. In Proceedings of the Seventh International Conference on Solid State Lighting ICSSL7, San Diego, CA, USA, 27–29 August 2007; SPIE: San Diego, CA, USA, 2007; Volume 6669, pp. 53–64.
127. Vishnuram, P.; Narayanamoorthi, R.; Vijayakumar, K.; Bajaj, M.; Shouran, M.; Samad, B.A.; Kamel, S. A comprehensive review on various non-isolated power converter topologies for a light-emitting diode driver. *Front. Energy Res.* **2022**, *10*, 1055258. [CrossRef]
128. Phan, D.T.; Mondal, S.; Tran, L.H.; Thien, V.T.M.; Van Nguyen, H.; Nguyen, C.H.; Park, S.; Choi, J. A flexible, and wireless LED therapy patch for skin wound photomedicine with IoT-connected healthcare application. *Flex. Print. Electron.* **2021**, *6*, 045002. [CrossRef]
129. Pearton, S.J.; Kang, B.S.; Kim, S.; Ren, F.; Gila, B.P.; Abernathy, C.R.; Lin, J. GaN-based diodes and transistors for chemical, gas, biological and pressure sensing. *J. Phys. Condens. Matter* **2004**, *16*, R961. [CrossRef]
130. Chen, H.; Yeh, T.H.; He, J.; Zhang, C.; Abbel, R.; Hamblin, M.R.; Huang, Y.; Lanzafame, R.J.; Stadler, I.; Celli, J.; et al. Flexible quantum dot light-emitting devices for targeted photo medical applications. *J. Soc. Inf. Disp.* **2018**, *26*, 296–303. [CrossRef] [PubMed]
131. Jeon, Y.; Noh, I.; Seo, Y.C.; Han, J.H.; Park, Y.; Cho, E.H.; Choi, K.C. Parallel-stacked flexible organic light-emitting diodes for wearable photodynamic therapeutics and color-tunable optoelectronics. *ACS Nano* **2020**, *14*, 15688–15699. [CrossRef]
132. Cho, I.H.; Anoop, G.; Suh, D.W.; Lee, S.J.; Yoo, J.S. On the stability and reliability of $Sr_{1-x}Ba_xSi_2O_2N_2$:Eu^{2+} phosphors for white LED applications. *Opt. Mater. Express* **2012**, *2*, 1292–1305. [CrossRef]
133. Anoop, G.; Kim, K.P.; Suh, D.W.; Cho, I.H.; Yoo, J.S. Optical Characteristics of $Sr_2Si_3O_2N_4$:Eu^{2+} Phosphors for White Light Emitting Diodes. *Electrochem. Solid-State Lett.* **2011**, *14*, J58. [CrossRef]
134. Taguchi, T. Technical trends and future view of white LED lighting, Headline Review. *OHM* **2004**, *5*, 8–9.
135. Taguchi, T. Present Status of Energy Saving Technologies and Future Prospect in White LED Lighting. *IEEJ Trans. Electr. Electron. Eng.* **2007**, *3*, 21–26. [CrossRef]
136. Bergh, A.; Craford, G.; Duggal, A.; Haitz, R. The Promise and Challenge of Solid-State Lighting. *Phys. Today* **2001**, *54*, 42–47. [CrossRef]
137. LED Lighting Market Size, Share & Growth Report, 2020–2030 Industry Report. Available online: https://www.grandviewresearch.com/industry-analysis/led-lighting-market (accessed on 15 September 2023).
138. Tang, C.W.; VanSlyke, S.A. Organic electroluminescent diodes. *Appl. Phys. Lett.* **1987**, *51*, 913–915. [CrossRef]
139. Kulkarni, A.P.; Tonzola, C.J.; Babel, A.; Jenekhe, S.A. Electron transport materials for organic light-emitting diodes. *Chem. Mater.* **2004**, *16*, 4556–4573. [CrossRef]
140. Cole, C.M.; Kunz, S.V.; Baumann, T.; Blinco, J.P.; Sonar, P.; Barner-Kowollik, C.; Yambem, S.D. Flexible Inkjet Printed Polymer Light-Emitting Diodes using a Self-Hosted Non-Conjugated TADF Polymer. *Macromol. Rapid Commun.* **2023**, *44*, 2300015. [CrossRef] [PubMed]
141. Huang, C.C.; Xue, M.M.; Wu, F.P.; Yuan, Y.; Liao, L.S.; Fung, M.K. Deep-blue and hybrid-white organic light emitting diodes based on a twisting carbazole-benzofuro [2, 3-b] pyrazine fluorescent emitter. *Molecules* **2019**, *24*, 353. [CrossRef]
142. Xu, Z.; Yu, D.; Yu, M. Synthesis and photophysical properties of novel 4-aryl substituted thiophen derivatives with a vinyl-quinoline unit. *J. Chem. Res.* **2013**, *37*, 441–443. [CrossRef]
143. Mawphlang, O.I.L.; Kharshiing, E.V. Photoreceptor Mediated Plant Growth Responses: Implications for Photoreceptor Engineering toward Improved Performance in Crops. *Front. Plant Sci.* **2017**, *8*, 268784. [CrossRef]
144. Bula, R.J.; Morrow, R.C.; Tibbitts, T.W.; Barta, D.J.; Ignatius, R.W.; Martin, T.S. Light-emitting Diodes as a Radiation Source for Plants. *HortScience* **1991**, *26*, 203–205. [CrossRef]
145. Hoenecke, M.E.; Bula, R.J.; Tibbitts, T.W. Importance of 'Blue' Photon Levels for Lettuce Seedlings Grown under Red-light-emitting Diodes. *HortScience* **1992**, *27*, 427–430. [CrossRef] [PubMed]
146. Deitzer, G.F.; Hayes, R.M.; Jabben, M. Kinetics and Time Dependence of the Effect of Far Red Light on the Photoperiodic Induction of Flowering in Wintex Barley. *Plant Physiol.* **1979**, *64*, 1015–1021. [CrossRef] [PubMed]
147. Morgan, D.C.; Smith, H. A systematic relationship between phytochrome-controlled development and species habitat, for plants grown in simulated natural radiation. *Planta* **1979**, *145*, 253–258. [CrossRef] [PubMed]
148. Blaauw, O.H.; Blaauw-Jansen, G. The phototropic responses of Avena coleoptiles. *Acta Bot. Neerl.* **1970**, *19*, 755–763. [CrossRef]

149. Schwartz, A.; Zeiger, E. Metabolic energy for stomatal opening. Roles of photophosphorylation and oxidative phosphorylation. *Planta* **1984**, *161*, 129–136. [CrossRef] [PubMed]
150. Whelan, H.T. NASA Light-Emitting Diodes for the Prevention of Oral Mucositis in Pediatric Bone Marrow Transplant Patients. *J. Clin. Laser Med. Surg.* **2002**, *20*, 319–324. [CrossRef] [PubMed]
151. Trelles, M.A. Phototherapy in anti-aging and its photobiologic basics: A new approach to skin rejuvenation. *J. Cosmet. Dermatol.* **2006**, *5*, 87–91. [CrossRef] [PubMed]
152. Khoury, J.G.; Goldman, M.P. Use of light-emitting diode photo modulation to reduce erythema and discomfort after intense pulsed light treatment of photodamage. *J. Cosmet. Dermatol.* **2008**, *7*, 30–34. [CrossRef]
153. Ashkenazi, H.; Malik, Z.; Harth, Y.; Nitzan, Y. Eradication of Propionibacterium acnes by its endogenic porphyrins after illumination with high intensity blue light. *FEMS Immunol. Med. Microbiol.* **2003**, *35*, 17–24. [CrossRef]
154. Ra, Y.H.; Rashid, R.T.; Liu, X.; Lee, J.; Mi, Z. Scalable nanowire photonic crystals: Molding the light emission of InGaN. *Adv. Funct. Mat.* **2017**, *27*, 1702364. [CrossRef]
155. Cheng, C.; Ning, L.; Ke, X.; Molokeev, M.S.; Wang, Z.; Zhou, G.; Chuang, Y.C.; Xia, Z. Designing high-performance LED phosphors by controlling the phase stability via a hetero valent substitution strategy. *Adv. Opt. Mat.* **2020**, *8*, 1901608. [CrossRef]
156. Liu, A.; Mukhin, I.S.; Islamova, R.M.; Tian, J. Flexible Perovskite Light-Emitting Diodes: Characteristics and Performance. *Adv. Funct. Mat.* **2023**, *14*, 2312209. [CrossRef]
157. Heilmeier, G.H.; Zanoni, L.A.; Barton, L.A. Dynamic scattering: A new electrooptic effect in certain classes of nematic liquid crystals. *Proc. IEEE* **1968**, *56*, 1162–1171. [CrossRef]
158. Soref, R.A. Transverse field effects in nematic liquid crystals. *Appl. Phys. Lett.* **1973**, *22*, 165–166. [CrossRef]
159. Lee, J.; Chen, C.; Lee, P.; Lin, H.; Leung, M.; Chiu, T.; Lin, C. Blue organic light-emitting diodes: Current status, challenges, and future outlook. *J. Mater. Chem. C* **2019**, *7*, 5874–5888. [CrossRef]
160. Geffroy, B.; Le Roy, P.; Prat, C. Organic light-emitting diode (OLED) technology: Materials, devices and display technologies. *Polym. Int.* **2006**, *55*, 572–582. [CrossRef]
161. Chen, H.; Tan, G.; Wu, S.-T. Ambient contrast ratio of LCDs and OLED displays. *Opt. Express* **2017**, *25*, 33643–33656. [CrossRef]
162. Lv, X.; Loo, K.H.; Lai, Y.M.; Tse, C.K. Energy-Saving Driver Design for Full-Color Large-Area LED Display Panel Systems. *IEEE Trans. Ind. Electron.* **2014**, *61*, 4665–4673. [CrossRef]
163. Goldman, D. The World is Running Out of Plasma TVs. CNNMoney. 30 October 2014. Available online: https://money.cnn.com/2014/10/30/technology/plasma-tv/index.html (accessed on 18 February 2024).
164. Tsujimura, T. *OLED Display Fundamentals and Applications*, 2nd ed.; John Wiley & Sons: Hoboken, NJ, USA, 2017.
165. Shafer, R. Mini-LED vs. Micro-LED—What Is the Difference? Display Ninja. 4 December 2023. Available online: https://www.displayninja.com/mini-led-vs-microled/ (accessed on 18 February 2024).
166. Seetzen, H.; Heidrich, W.; Stuerzlinger, W.; Ward, G.; Whitehead, L.; Trentacoste, M.; Ghosh, A.; Vorozcovs, A. High Dynamic Range Display Systems. In *Seminal Graphics Papers: Pushing the Boundaries*; Association for Computing Machinery: New York, NY, USA, 2023; Volume 2, pp. 39–47.
167. Daly, S.; Kunkel, T.; Sun, X.; Farrell, S.; Crum, P. 41.1: Distinguished Paper: Viewer Preferences for Shadow, Diffuse, Specular, and Emissive Luminance Limits of High Dynamic Range Displays. *SID Symp. Dig. Tech. Pap.* **2013**, *44*, 563–566. [CrossRef]
168. Jiang, H.X.; Jin, S.X.; Li, J.; Shakya, J.; Lin, J.Y. III-nitride blue micro displays. *Appl. Phys. Lett.* **2001**, *78*, 1303–1305. [CrossRef]
169. Tian, P.; McKendry, J.; Gu, E.; Chen, Z.; Sun, Y.; Zhang, G.; Dawson, M.; Liu, R. Fabrication, characterization and applications of flexible vertical InGaN micro-light emitting diode arrays. *Opt. Express* **2016**, *24*, 699–707. [CrossRef] [PubMed]
170. Global Micro-LED Market, Research and Markets. Available online: https://www.researchandmarkets.com/reports/5067415/global-micro-led-market-with-covid-19-impact (accessed on 15 December 2023).
171. Matthews, A. Micro-LED Displays Could Disrupt LCD and OLED Supply Chains. Electronic Specifier. 17 February 2017. Available online: https://www.electronicspecifier.com/products/displays/microled-displays-could-disrupt-lcd-and-oled-supply-chains (accessed on 17 December 2023).
172. Cok, R.; Meitl, M.; Rotzoll, R.; Melnik, G.; Fecioru, A.; Trindade, A.; Raymond, B.; Bonafede, S.; Gomez, D.; Moore, T.; et al. Inorganic light-emitting diode displays using micro-transfer printing. *J. Soc. Inf. Disp.* **2017**, *25*, 589–609. [CrossRef]
173. Corbett, B.; Loi, R.; Zhou, W.; Liu, D.; Ma, Z. Transfer print techniques for heterogeneous integration of photonic components. *Prog. Quantum Electron.* **2017**, *52*, 1–17. [CrossRef]
174. Zhuang, Z.; Guo, X.; Liu, B.; Hu, F.; Li, Y.; Tao, T.; Dai, J.; Zhi, T.; Xie, Z.; Chen, P.; et al. High Color Rendering Index Hybrid III-Nitride/Nanocrystals White Light-Emitting Diodes. *Adv. Funct. Mater.* **2015**, *26*, 36–43. [CrossRef]
175. Wu, T.; Sher, C.-W.; Lin, Y.; Lee, C.-F.; Liang, S.; Lu, Y.; Chen, S.-W.H.; Guo, W.; Kuo, H.-C.; Chen, Z. Mini-led and micro-led: Promising candidates for the next generation display technology. *Appl. Sci.* **2018**, *8*, 1557. [CrossRef]
176. Gu, Y.; Zhang, L.; Yang, J.K.W.; Yeo, S.P.; Qiu, C.-W. Color generation via subwavelength plasmonic nanostructures. *Nanoscale* **2015**, *7*, 6409–6419. [CrossRef] [PubMed]
177. Huang, Y.M.; Singh, K.; Liu, A.; Lin, C.; Chen, Z.; Wang, K.; Lin, Y.; Liu, Z.; Wu, T.; Kuo, H. Advances in Quantum-Dot-Based Displays. *Nanomaterials* **2020**, *10*, 1327. [CrossRef]
178. Yang, Z.; Gao, M.; Wu, W.; Yang, X.; Sun, X.; Zhang, J.; Wang, H.; Liu, R.; Han, C.; Yang, H.; et al. Recent advances in quantum dot-based light-emitting devices: Challenges and possible solutions. *Mater. Today* **2019**, *24*, 69–93. [CrossRef]

179. Huang, Y.; Hsiang, E.L.; Deng, M.Y.; Wu, S.T. Mini-LED, Micro-LED and OLED displays: Present status and future perspectives. *Light Sci. Appl.* **2020**, *9*, 105. [CrossRef]
180. Liu, X.; Tong, C.; Luo, X.; Li, W.; Liu, Z. P-6.8: Study of mass transfer for micro-LED manufacturing. *SID Symposium Dig. Tech. Pap.* **2019**, *50*, 775–778. [CrossRef]
181. Zhao, H.; Yan, Q.; Wang, J.; Hua, D.X. A Compound Parabolic Concentrator Coupled to an Optical Microlenslet Array for Projection Display. In *MME 2016*; Atlantis Press: Amsterdam, The Netherlands, 2016; pp. 566–572.
182. Water | WHO | Regional Office for Africa. 16 May 2024. Available online: https://www.afro.who.int/health-topics/water (accessed on 18 May 2024).
183. *Ultraviolet Disinfection Guidance Manual for the Final Long Term 2 Enhanced Surface Water Treatment Rule*; U.S Environmental Protection Agency: Washington, DC, USA, 2006. Available online: https://www.epa.gov/system/files/documents/2022-10/ultraviolet-disinfection-guidance-manual-2006.pdf (accessed on 19 December 2023).
184. Sergejevs, A.; Clarke, C.T.; Allsopp, D.W.E.; Marugan, J.; Jaroenworaluck, A.; Singhapong, W.; Manpetch, P.; Timmers, R.; Casado, C.; Bowen, C.R. A calibrated UV-LED based light source for water purification and characterization of photocatalysis. *Photochem. Photobiol. Sci.* **2017**, *16*, 1690–1699. [CrossRef] [PubMed]
185. Chevremont, A.C.; Boudenne, J.-L.; Coulomb, B.; Farnet, A.-M. Impact of watering with UV-LED-treated wastewater on microbial and physico-chemical parameters of soil. *Water Res.* **2013**, *47*, 1971–1982. [CrossRef]
186. Chevremont, A.C.; Farnet, A.M.; Coulomb, B.; Boudenne, J.L. Effect of coupled UV-A and UV-C LEDs on both microbiological and chemical pollution of urban wastewaters. *Sci. Total Environ.* **2012**, *426*, 304–310. [CrossRef] [PubMed]
187. Buonanno, M.; Randers-Pehrson, G.; Bigelow, A.W.; Trivedi, S.; Lowy, F.D.; Spotnitz, H.M.; Hammer, S.M.; Brenner, D.J. 207-nm UV Light—A Promising Tool for Safe Low-Cost Reduction of Surgical Site Infections. I: In Vitro Studies. *PLoS ONE* **2013**, *8*, e76968. [CrossRef]
188. Buonanno, M.; Ponnaiya, B.; Welch, D.; Stanislauskas, M.; Pehrson, G.R.; Smilenov, L.; Lowy, F.D.; Owens, D.M.; Brenner, D.J. Germicidal efficacy and mammalian skin safety of 222-nm UV light. *Radiat. Res.* **2017**, *187*, 493–501. [CrossRef] [PubMed]
189. Oguma, K.; Kita, R.; Sakai, H.; Murakami, M.; Takizawa, S. Application of UV light emitting diodes to batch and flow-through water disinfection systems. *Desalination* **2013**, *328*, 24–30. [CrossRef]
190. de Carvalho, N.A.; Stachler, E.N.; Cimabue, N.; Bibby, K. Evaluation of Phi6 persistence and suitability as an enveloped virus surrogate. *Environ. Sci. Technol.* **2017**, *51*, 8692–8700. [CrossRef] [PubMed]
191. Turgeon, N.; Toulouse, M.-J.; Martel, B.; Moineau, S.; Duchaine, C. Comparison of five bacteriophages as models for viral aerosol studies. *Appl. Environ. Microbiol.* **2014**, *80*, 4242–4250. [CrossRef]
192. Bhattarai, T.; Ebong, A.; Raja, M.Y.A.; Munir, M. Advancements in 275 nm UV-LED Technology for Deactivation of Bacteriophages, Phi6 and MS2. In Proceedings of the 2023 IEEE HONET, 20th International Conference on Smart Communities, Boca Raton, FL, USA, 4–6 December 2023; pp. 120–125.
193. Aoyagi, Y.; Takeuchi, M.; Yoshida, K.; Kurouchi, M.; Yasui, N.; Kamiko, N.; Araki, T.; Nanishi, Y. Inactivation of Bacterial Viruses in Water Using Deep Ultraviolet Semiconductor Light-Emitting Diode. *J. Environ. Eng.* **2011**, *137*, 1215–1218. [CrossRef]
194. Bowker, C.; Sain, A.; Shatalov, M.; Ducoste, J. Microbial UV fluence-response assessment using a novel UV-LED collimated beam system. *Water Res.* **2011**, *45*, 2011–2019. [CrossRef]
195. Tseng, C.C.; Li, C.-S. Inactivation of viruses on surfaces by ultraviolet germicidal irradiation. *J. Occup. Environ. Hyg.* **2007**, *4*, 400–405. [CrossRef]
196. Beck, S.E.; Ryu, H.; Boczek, L.A.; Cashdollar, J.L.; Jeanis, K.M.; Rosenblum, J.S.; Lawal, O.R.; Linden, K.G. Evaluating uv-c led disinfection performance and investigating potential dual-wavelength synergy. *Water Res.* **2017**, *109*, 207–216. [CrossRef] [PubMed]
197. Mamane, H.; Shemer, H.; Linden, K.G. Inactivation of *E. coli*, *B. subtilis* spores, and MS2, T4, and T7 phage using UV/H_2O_2 advanced oxidation. *J. Hazard. Mater.* **2007**, *146*, 479–486. [CrossRef] [PubMed]
198. Bar-On, Y.M.; Flamholz, A.; Phillips, R.; Milo, R. Science forum: Sars-cov-2 (COVID-19) by the numbers. *eLife* **2020**, *9*, e57309. [CrossRef] [PubMed]
199. Silverman, A.I.; Boehm, A.B. Systematic review and meta-analysis of the persistence and disinfection of human coronaviruses and their viral surrogates in water and wastewater. *Environ. Sci. Technol. Lett.* **2020**, *7*, 544–553. [CrossRef] [PubMed]
200. Bhattarai, T.; Raja, M.Y.A.; Ebong, A.; Bhutta, M.K. On the nano-engineered III-nitride quantum-wells-based deep-UV light emitting diodes for COVID disinfection applications. In Proceedings of the Second iiScience International Conference 2021: Recent Advances in Photonics and Physical Sciences, Faisalabad, Pakistan, 29–30 March 2021; SPIE: Bellingham, WA, USA, 2021; Volume 11877, pp. 61–66.
201. Buonanno, M.; Stanislauskas, M.; Ponnaiya, B.; Bigelow, A.W.; Randers-Pehrson, G.; Xu, Y.; Shuryak, I.; Smilenov, L.; Owens, D.M.; Brenner, D.J. 207-nm UV light—A promising tool for safe low-cost reduction of surgical site infections. ii: In-vivo safety studies. *PLoS ONE* **2016**, *11*, e0138418. [CrossRef] [PubMed]
202. Cooke, M. GaN:AlN Superlattice UVC LEDs Boost Light Extraction. Semiconductor-Today. 24 August 2023. Available online: https://www.semiconductor-today.com/news_items/2023/aug/silanna-240823.shtml (accessed on 17 December 2023).
203. Nicholls, J.; Anderson, L.; Lee, W.; Ahn, J.J.S.; Baskaran, A.; Bang, H.; Belloeil, M.; Cai, Y.; Campbell, J.; Chai, J.; et al. High performance and high yield sub-240 nm AlN: GaN short period superlattice LEDs grown by MBE on 6 in. sapphire substrates. *Appl. Phys. Lett.* **2023**, *123*, 051105. [CrossRef]

204. Kumar, G.D.; Mishra, A.; Dunn, L.; Townsend, A.; Oguadinma, I.C.; Bright, K.R.; Gerba, C.P. Biocides and novel antimicrobial agents for the mitigation of coronaviruses. *Front. Microbiol.* **2020**, *11*, 1351.
205. Hijnen, W.; Beerendonk, E.; Medema, G.J. Inactivation credit of UV radiation for viruses, bacteria and protozoan (oo) cysts in water: A review. *Water Res.* **2006**, *40*, 3–22. [CrossRef]
206. Buonanno, M.; Welch, D.; Shuryak, I.; Brenner, D.J. Far-UVC light (222 nm) efficiently and safely inactivates airborne human coronaviruses. *Sci. Rep.* **2020**, *10*, 1–8.
207. Bedell, K.; Buchaklian, A.H.; Perlman, S. Efficacy of an automated multiple emitter whole-room ultraviolet-c disinfection system against coronaviruses MHV and MERS-CoV. *Infect. Control Hosp. Epidemiol.* **2016**, *37*, 598–599. [CrossRef] [PubMed]
208. Bucknall, R.A.; King, L.M.; Kapikian, A.Z.; Chanock, R.M. Studies with human coronaviruses ii. some properties of strains 229e and oc43. *Proc. Soc. Exp. Biol. Med.* **1972**, *139*, 722–727. [CrossRef] [PubMed]
209. Kariwa, H.; Fujii, N.; Takashima, I. Inactivation of SARS coronavirus by means of povidone-iodine, physical conditions, and chemical reagents. *Jpn. J. Vet. Res.* **2004**, *52*, 105–112. [CrossRef] [PubMed]
210. Gerchman, Y.; Mamane, H.; Friedman, N.; Mandelboim, M. UV-led disinfection of coronavirus: Wavelength effect. *J. Photochem. Photobiol. B Biol.* **2020**, *212*, 112044. [CrossRef]
211. Ansaldi, F.; Banfi, F.; Morelli, P.; Valle, L.; Durando, P.; Sticchi, L.; Contos, S.; Gasparini, R.; Crovari, P. Sars-CoV, influenza A and syncytial respiratory virus resistance against common disinfectants and ultraviolet irradiation. *J. Prev. Med. Hyg.* **2004**, *45*, 5–8.

Disclaimer/Publisher's Note: The statements, opinions and data contained in all publications are solely those of the individual author(s) and contributor(s) and not of MDPI and/or the editor(s). MDPI and/or the editor(s) disclaim responsibility for any injury to people or property resulting from any ideas, methods, instructions or products referred to in the content.